


Towards a solution to the H_0 tension

Axel de la Macorra^{*,} Joanna Garrido,[†] and Erick Almaraz[‡]

Instituto de Física, Universidad Nacional Autónoma de México, Ciudad de México, C.P. 04510, México

 (Received 29 July 2021; accepted 22 October 2021; published 24 January 2022)

The tension between the current expansion rate H_0 using *Planck* data and direct model-independent measurements in the local Universe has grown in the context of the Λ CDM model. The growing tension among early-time and local measurements of H_0 has not ameliorated and remains a crucial and open question in cosmology. Solutions to understanding this tension are possible hidden sources of systematic error in the observable measurements or modifications to the concordance Λ CDM model. In this work, we investigate a solution to the H_0 tension by modifying Λ CDM and we add at early times an extra-relativistic energy density ρ_{ex} beyond the standard model. For a scale factor larger than a_c , this extra energy density ρ_{ex} dilutes faster than radiation and becomes subdominant. In some contexts, this ρ_{ex} corresponds to early dark energy or bound dark energy, and we refer to this cosmological model as Λ CDM-Nx. We implement Λ CDM-Nx in CAMB and perform a full COSMOMC analysis, allowing to simultaneously fit the latest data from cosmic microwave background (CMB) anisotropies and the value of $H_0 = 74.03 \pm 1.42 \text{ km s}^{-1} \text{ Mpc}^{-1}$ obtained from distance ladder measurements using Cepheid variables to calibrate the absolute luminosity of type Ia supernovae by Riess *et al.* [*Astrophys. J.* **876**, 85 (2019)]. The inclusion of ρ_{ex} ameliorates the tension between early- and late-time measurements only slightly, and we obtain a value $H_0 = (68.70 \pm 0.45 \text{ km s}^{-1} \text{ Mpc}^{-1})$ which is still in conflict with local measurements. We follow up our analysis by proposing two forecasting standard deviations $\sigma_H = 1$ and $\sigma_H = 0.5$ (in units of $\text{km s}^{-1} \text{ Mpc}^{-1}$) for local distance measurements, i.e., $H_0 = (74.03 \pm 1)$ and $H_0 = (74.03 \pm 0.5) \text{ km s}^{-1} \text{ Mpc}^{-1}$. We implement these new values of H_0 in COSMOMC including CMB and Riess data, and we obtain a value of $H_0 = (72.83 \pm 0.47) \text{ km s}^{-1} \text{ Mpc}^{-1}$ at the 68% confidence level for $\sigma_H = 0.5$, which is fully consistent with Riess' results, while the price to pay is a percentage increase of the reduced CMB $(\chi_{\text{CMB}}^{\text{red}})^2$ of 0.127% vs the Λ CDM model, corresponding to a very small increase. Finally, the energy density ρ_{ex} leaves distinctive imprints in the matter power spectrum at scales $k \sim k_c$ [with $k_c = a_c H(a_c)$] and in the CMB power spectrum, allowing for independent verification of our analysis.

DOI: [10.1103/PhysRevD.105.023526](https://doi.org/10.1103/PhysRevD.105.023526)

I. OVERVIEW

Even before the discovery of the accelerated expansion rate of the Universe [1–3], the quest to determine the rate of expansion of the Universe occupied a central role in cosmology for decades. However, great technical and observational achievements in recent years have delivered percent-level precision measurements of the cosmological parameters. The improvement in probing the physics of different epochs of the Universe has yielded discordance in some measurements. In particular, we have an increasing tension among the values of some cosmological parameters, such as the value of H_0 .

According to the distance ladder measurements, which use nearby Cepheids to anchor supernovae data and

determine their distance [4–6], the obtained value for the Hubble parameter is up to 3.4σ higher than the value determined using cosmic microwave background (CMB) probes. This distance ladder method to determine H_0 is model independent, i.e., it does not rely on the underlying cosmological model, and the latest estimate reported a value of $H_0 = 74.03 \pm 1.42 \text{ km s}^{-1} \text{ Mpc}^{-1}$ [4].

An alternative calibration of the distance ladder uses the tip of the red giant branch method [7]. This method is independent of the Cepheid distance scale and gives a value of $H_0 = 69.8 \pm 1.9 \text{ km s}^{-1} \text{ Mpc}^{-1}$ [8], which is in the middle of the range defined by the current Hubble tension. It agrees at the 1.2σ level with that of the *Planck* Collaboration [9], and at the 1.7σ level with the SHOES measurement of H_0 based on the Cepheid distance scale [4]. Measurements of lensing time delays [10–12] between multiple images of background quasars provide a high value for H_0 which is in agreement with the traditional local distance ladder estimation. Reference [10]

*macorra@fisica.unam.mx

†joannagarr@ciencias.unam.mx

‡ealmaraz@estudiantes.fisica.unam.mx

reported a value of $H_0 = 71.9^{+2.4}_{-3.0} \text{ km s}^{-1} \text{ Mpc}^{-1}$, while Ref. [11] found the value $H_0 = 72.5^{+2.1}_{-2.3} \text{ km s}^{-1} \text{ Mpc}^{-1}$ and the H0LiCOW team [12] reported $H_0 = 73.3^{+1.7}_{-1.8} \text{ km s}^{-1} \text{ Mpc}^{-1}$ by making a joint analysis of six gravitationally lensed quasars with measured time delays. This technique is completely independent of both the supernovae and CMB analyses.

The precise CMB measurements by *Planck* [9] (hereafter [P18]) provided a value of the Hubble parameter $H_0 = (67.27 \pm 0.60) \text{ km s}^{-1} \text{ Mpc}^{-1}$ at the 68% confidence level assuming the standard Λ CDM model, corresponding to the particle content of the standard model of particles physics [13] supplemented by cold dark matter and a cosmological constant as dark energy. The value of H_0 from CMB measurements is in conflict with the value of H_0 determined at late cosmological times from local measurements by Riess *et al.* [4] (hereafter [R19]) given by $H_0 = (74.03 \pm 1.42) \text{ km s}^{-1} \text{ Mpc}^{-1}$ and with an average reported value $H_0 = (73.3 \pm 0.8) \text{ km s}^{-1} \text{ Mpc}^{-1}$ [14] from different local measurements projects. A combined analysis of distance measurements for four megamaser-hosting galaxies done by the Megamaser Cosmology Project [15] gave the value $H_0 = 73.9 \pm 3.0 \text{ km s}^{-1} \text{ Mpc}^{-1}$. A combination of “time-delay cosmography” [16] and the distance ladder results gives a result of $H_0 = 74.5^{+5.6}_{-6.1} \text{ km s}^{-1} \text{ Mpc}^{-1}$.

On the other hand, the latest results from the *Planck* Collaboration report a model-dependent Λ CDM extrapolated value of $H_0 = (67.36 \pm 0.54) \text{ km s}^{-1} \text{ Mpc}^{-1}$ [9], while the latest results from the Atacama Cosmology Telescope [17] CMB probe found a value that agrees with the *Planck* satellite estimate within 0.3%, reporting a value of $H_0 = 67.6 \pm 1.5 \text{ km s}^{-1} \text{ Mpc}^{-1}$. In a recent review, Verde *et al.* reported an average value of local measurements of $H_0 = 73.03 \pm 0.8 \text{ km s}^{-1} \text{ Mpc}^{-1}$ [14]. Regardless of the exact value of H_0 obtained from local measurements, the significance of the tension between the measurements of early and late times lies in the range $4.0 - 5.7\sigma$ [14], implying some profound misunderstanding in either the systematic errors of the observational analysis or the theoretical Λ CDM model.

The discrepancy between the early- and late-Universe H_0 measurements has gained major attention from the cosmological community, and some authors have explored a variety of extensions to the minimal Λ CDM model to accommodate the high value of H_0 obtained from local measurements with the precise information encoded in the CMB. Trying to understand the tension between these two values led to a reexamination of possible sources of systematic errors in the observations [18–20], but it also suggests the need to extend our physical model describing the Universe. Any of these theoretical modifications should leave the accurate determination of the angular scale of the acoustic peaks in the CMB power spectrum by *Planck* unchanged [21].

The H_0 tension has been studied recently in Refs. [22–26], and more recently in Refs. [27–34] where the impact on structure formation was studied.

The suggestion made in Ref. [5] to explore the existence of dark radiation in the early Universe in the range of $\Delta N_{\text{eff}} = 0.4 - 1$ to solve this tension was explored in detail in Ref. [35], where they explored changing the values of N_{eff} and c_s . Alternatively, some models explore the possibility of having interactions within the dark sector (dark matter and dark energy) so that can not only help to solve the cosmic coincidence problem, but also solve the H_0 tension [36,37]. In the context of exploring alternative models for the dark sector, Ref. [38] investigated the possible scenarios for a phantom crossing dark energy component as another option for solving the Hubble tension. Given the amount of interest invested in this topic, some authors have explored changes to general relativity in order to accommodate the high value of H_0 with CMB data. For instance, Ref. [39] explored a model in which a fifth force between dark matter particles is mediated by a scalar field which plays the role of dark energy. Models that vary the effective gravitational constant and effective number of relativistic degrees of freedom are explored in Ref. [40]. In a different approach, Ref. [41] explored the possibility of strongly interacting massive neutrinos to alleviate the H_0 tension.

However, perhaps the most widely explored extension to Λ CDM is known as early dark energy (EDE) [42–45]. There is no unique or unambiguous definition of EDE. Typically, in EDE models there is an early period during which an extra energy component—not contained in the Λ CDM model—contributes to the expansion rate of the Universe H . Even the terminology of “early period” is model and case dependent as it can take place in the radiation-dominated era or at late times, such as at $z \sim 4$. Original EDE models were motivated by the evolution of scalar fields (quintessence) to describe the evolution of dark energy [42,43,46–48]. These EDE models had in general a non-negligible energy density at early times, well within the radiation-dominated era. The equation of state w of the quintessence scalar field had a period of $w = 1/3$ at early times, with a later transition to $w \sim 1$, diluting the energy density and becoming subdominant for a long period of time covering most of the matter-dominated era, to finally reappear dynamically at late times as dark energy [49–56]. Alternatively, recent EDE models add an extra component to the energy-momentum tensor $\Omega_{\text{EDE}}(a)$ at different scales, and this EDE dilutes rapidly at a scale factor a_c , which determines the time of the transition, with $\Omega_{\text{EDE}} = 0$ for $a \gg a_c$. This EDE modifies the expansion rate of the universe, the cosmological distances and the density perturbations at different epochs [44,57] and some EDE models [22,58,59] have been proposed as deviations from Λ CDM and possible solutions to the H_0 crisis [4].

Furthermore, the increasing statistical tension in the estimated Hubble parameter from early- and late-time

observations [14] has reignited interest in alternative cosmological models, while the surge in clustering data [60] and the percentage precision for cosmic distances [9,60] allows to search for extensions beyond Λ CDM by searching for cosmological features in the matter [25,33,43,44,57,58,61] or CMB power spectra, standard distances rulers, or tensions in the Λ CDM model such as the recent H_0 crisis [4].

On the other hand, a physically motivated dark energy model presented in Refs. [52,62–64] introduces a dark sector, corresponding to a dark gauge group SU(3) similar to the strong QCD interaction in the standard model. The fundamental particles contained in this dark SU(3) are massless and redshift as radiation for $a < a_c$, but the underlying dynamics of the gauge interaction of this group forms massive bound states once the interaction becomes strong, similarly to protons and neutrons in the strong QCD force, and we refer to this model as the “bound dark energy” (BDE) model [52,62,63]. The energy of the elementary particles is transferred to the lightest bound state after the phase transition takes place at a_c and corresponds to a scalar field ϕ . Due to the dynamics of ϕ , the energy density of BDE dilutes at a_c and eventually reappears close to the present time as dark energy [62,63]. This dilution at a_c leaves interesting imprints on the matter power spectrum [64] (for a model-independent analysis see, for instance, Refs. [65,66]). BDE is a particular model of elementary particle physics where an extra gauge group SU(3) is introduced and naturally contains the main characteristics of EDE, namely, it accounts for an extra-relativistic energy density ρ_{ex} at high energies, while $\rho_{\text{ex}}(a)$ dilutes rapidly for $a > a_c$ due to a phase transition of the underlying gauge and forms bound states [62,63].

The main goal of this work is to study the tension in and possible solution to the value of H_0 from low-redshift probes with the precise determination of CMB data. This paper is organized as follows. In Sec. II we present a brief introduction, and we give the details behind our modifications through toy model calculations in Sec. III. We implement EDE models in the Boltzmann code CAMB and in COSMOMC, as well as a discussion of our results, are presented in Sec. IV, and we describe the analysis in Sec. IVA. In Sec. V we present our conclusions.

II. INTRODUCTION

The main goal of this work is to study the tension in and possible solutions to the value of H_0 from low-redshift probes and the precise determination of CMB data. We work with two different cosmological models: the first one is simply the standard Λ CDM model, corresponding to the content of the standard model of particles physics [13], cold dark matter, and a cosmological constant as dark energy, while the second model we denote as Λ CDM-Nx, corresponding to Λ CDM but supplemented with an extra-relativistic energy density $\rho_{\text{ex}}(a) \sim 1/a^3$ present at a scale

factor $a \leq a_c$, while for $a > a_c$ $\rho_{\text{ex}}(a)$ dilutes as $\rho_{\text{ex}}(a) \sim 1/a^6$. This model Λ CDM-Nx is inspired by BDE [62,63].

For definiteness, in this study we take the recent local measurement $H_0 = (74.03 \pm 1.42) \text{ km s}^{-1} \text{ Mpc}^{-1}$ at the 68% confidence level from [R19], and the inferred value of $H_0 = (67.27 \pm 0.60) \text{ km s}^{-1} \text{ Mpc}^{-1}$ at the 1σ level from the *Planck* 2018 data [P18] for a Λ CDM model using (TT, TE, EE + LowE) measurements. We modified CAMB [67,68] and perform a full COSMOMC analysis¹ [69–71]. We perform the analysis for the Λ CDM and Λ CDM-Nx models. However, besides the 1σ value $\sigma_H = 1.42$ from local H_0 measurements [R19], we also consider two forecasting 1σ values σ_H , and for definiteness we choose and introduce in the analysis the value $H_0 = 74.03 \pm \sigma_H \text{ km s}^{-1} \text{ Mpc}^{-1}$, with $\sigma_H = 1$ and $\sigma_H = 0.5$ (in units of $\text{km s}^{-1} \text{ Mpc}^{-1}$). With these two forecasting values we assess the impact of more precise local H_0 measurements on the posterior value of H_0 from CMB + local H_0 data. Notice, however, that our forecasting 1σ 's $\sigma_H = 1$ and $\sigma_H = 0.5$ are similar to the one reported in Ref. [14] with $H_0 = (73.03 \pm 0.8) \text{ km s}^{-1} \text{ Mpc}^{-1}$. The results of our analysis are shown in Sec. IVA and we present the conclusions in Sec. V.

The value of $H_0 = 74.03 \pm 1.42 \text{ km s}^{-1} \text{ Mpc}^{-1}$ determined by Riess *et al.* [R19] [4–6] has a discrepancy of between 4.0σ and 5.8σ [14] with the value inferred from *Planck* CMB (TT, TE, EE + LowE) data [P18], $H_0 = (67.27 \pm 0.60) \text{ km s}^{-1} \text{ Mpc}^{-1}$, at the 1σ level in the Λ CDM model. The solution to this discrepancy remains an open question in cosmology. Since CMB radiation is generated at an early epoch $a_* = 1/1090$, the prediction of the Hubble constant at the present time H_0 inferred from *Planck* data is a consequence of the assumption of the validity of the standard Λ CDM model. So, either *Planck* or local H_0 measurements are inaccurate, due to possible systematics, or we need to modify the concordance cosmological Λ CDM model. Here we follow this second option and attempt to reconcile the value of H_0 from these two observational experiments.

We work with two different cosmological models. The first one is simply the standard Λ CDM model, corresponding to the content of the standard model of particles physics [13] and a cosmological constant as dark energy. We name the second model Λ CDM-Nx and it consists of Λ CDM supplemented by an extra-relativistic energy density $\rho_{\text{ex}}(a) \sim 1/a^3$ present at early times for a scale factor $a \leq a_c$, where a_c denotes the transition scale factor, and we assume that $\rho_{\text{ex}}(a) \sim 1/a^6$ for $a > a_c$, motivated by BDE and EDE models.

We have implemented the cosmological Λ CDM-Nx model in CAMB [67,68] and we perform a full

¹<http://cosmologist.info/cosmomc>.

COSMOMC analysis for several data sets described in Sec. IV for both Λ CDM and Λ CDM-Nx models, and we present the results in Secs. IV A and IV B and conclusions in Sec. V.

For definiteness, we take the (TT, TE, EE + lowE) measurements from *Planck* 2018 [P18] with $H_0 = (67.27 \pm 0.60) \text{ km s}^{-1} \text{ Mpc}^{-1}$ and the recent local measurement $H_0 = (74.03 \pm 1.42) \text{ km s}^{-1} \text{ Mpc}^{-1}$ at the 68% confidence level from [R19]. However, besides the 1σ value $\sigma_H = 1.42$ (in units of $\text{km s}^{-1} \text{ Mpc}^{-1}$) from local measurements [R19], we also introduce two forecasting 1σ values and we choose $\sigma_H = 1$ and $\sigma_H = 0.5$. With these two forecasting values of σ_H , i.e. $H_0 = 74.03 \pm \sigma_H$, we want to assess the impact of a more precise local H_0 measurements combined with CMB data on the posterior value of H_0 . Notice, however, that our forecasting 1σ values $\sigma_H = 1$ and $\sigma_H = 0.5$ are of the same order as the average value $H_0 = (73.03 \pm 0.8) \text{ km s}^{-1} \text{ Mpc}^{-1}$ reported in Ref. [14]. The results of these analyses are shown in Sec. IV A and we present our conclusions in Sec. V.

We will implement cosmological models Λ CDM and Λ CDM-Nx in CAMB and COSMOMC in Sec. IV, however we would like to present first a simple toy model in Sec. III illustrating how an extra-relativistic energy density $\rho_{\text{ex}}(a)$, present only at early times $a < a_c$, can account for the same acoustic scale $\theta(a_*)$ as measured by *Planck* [P18] but with the value of H_0 consistent with [R19]. We estimate the cosmological constraints analytically in Sec. III B and study the impact of the extra ρ_{ex} on the growth of the linear matter density and matter power spectrum in Sec. III C.

III. COSMOLOGICAL TOY MODELS

We now present a simple toy model to analytically illustrate how adding an extra-relativistic energy density $\rho_{\text{ex}}(a)$, present at early times, can account for having the same acoustic scale $\theta(a_*)$ as the Λ CDM model but with a higher value of H_0 .

A. Acoustic scale

The *Planck* satellite [9] has delivered impressive quality cosmological data by measuring the CMB background radiation. Perhaps the most accurate measurements are the acoustic scale anisotropies given by the acoustic angle θ , defined as the ratio of the comoving sound horizon $r_s(a_*)$ and the comoving angular diameter distance $D_A(a_*)$ evaluated at the recombination scale factor a_* (with a redshift $z_* = 1/a_* - 1 \simeq 1089$) as

$$\theta(a_*) = \frac{r_s(a_*)}{D_A(a_*)}. \quad (1)$$

The (TT, TE, EE + lowE) CMB *Planck* 2018 [9] measurements at the 68% confidence level give

$$100 \theta(a_*) = (1.04109 \pm 0.0003) \quad (2)$$

in the context of the standard Λ CDM model, corresponding to a flat Universe with CDM, a cosmological constant Λ as dark energy, and the standard model particles [13]. The comoving angular diameter distance and the acoustic scale are defined as

$$D_A(a_*) = \int_{a_*}^{a_o} \frac{da}{a^2 H(a)}, \quad r_s(a_*) = \int_{a_i}^{a_*} \frac{c_s}{a^2 H(a)} da, \quad (3)$$

where $H(a) \equiv \dot{a}/a$ is the Hubble parameter, a_o is the present-time scale factor (usually taken as $a_o = 1$), and c_s is the sound speed,

$$c_s(a) = \frac{1}{\sqrt{3(1+R)}}, \quad R \equiv \frac{3\rho_b}{4\rho_\gamma} = \frac{3}{4} \left(\frac{\Omega_{b0}}{\Omega_{\gamma0}} \right) \left(\frac{a}{a_o} \right). \quad (4)$$

Since *Planck* CMB measurements accurately determine the acoustic angle $\theta(a_*) = r_s(a_*)/D_A(a_*)$, any modification of Λ CDM must clearly preserve the ratio in $\theta(a_*)$. A larger value of H_0 reduces $D_A(a_*)$ and $r_s(a_*)$; however, since the integration limits differ in $D_A(a_*)$ and $r_s(a_*)$, a change in H_0 will modify the angle $\theta(a_*)$.

Let us take two models: the standard Λ CDM model (or “sm”), and Λ CDM-Nx (also referred as “smx”) corresponding to a Λ CDM with additional relativistic particles for $a < a_*$. Imposing the constraint to have the same acoustic scale $\theta(a_*)$ in these two models, i.e.,

$$\theta(a_*) = \frac{r_s^{\text{sm}}(a_*)}{D_A^{\text{sm}}(a_*)} = \frac{r_s^{\text{smx}}(a_*)}{D_A^{\text{smx}}(a_*)}, \quad (5)$$

the relative quotients of $r_s(a_*)$ and $D_A(a_*)$ of these models must satisfy

$$\xi \equiv \frac{D_A^{\text{smx}}(a_*)}{D_A^{\text{sm}}(a_*)} = \frac{r_s^{\text{smx}}(a_*)}{r_s^{\text{sm}}(a_*)}. \quad (6)$$

Any change in $D_A(a_*)^{\text{smx}}/D_A^{\text{sm}}(a_*)$ due, for example, to a different amount of H_0 can be compensated with a change in $r_s(a_*)^{\text{smx}}/r_s(a_*)^{\text{sm}}$ to maintain the same $\theta(a_*)$.

We impose the constraint to have the same acoustic scale $\theta(a_*)$ in both models, with Λ CDM (i.e., “sm”) having a value of H_0 as measured by *Planck* 2018 [P18], where we take for presentation purposes $H_0^P = 67$ (in units of $\text{km s}^{-1} \text{ Mpc}^{-1}$), and the second model Λ CDM-Nx (i.e., “smx”), corresponding to the standard Λ CDM model with extra-relativistic energy density $\rho_{\text{ex}}(a)$ and an H_0 given by $H_0^R = 74$ (in units of $\text{km s}^{-1} \text{ Mpc}^{-1}$), consistent with [R19]. We define the Hubble parameter in Λ CDM as $H_{\text{sm}}^2 = (8\pi G/3)\rho_{\text{sm}}$ with an energy content $\rho_{\text{sm}} = \rho_r^{\text{sm}} + \rho_m^{\text{sm}} + \rho_\Lambda^{\text{sm}}$ for radiation, matter, and the cosmological constant, respectively, while Λ CDM-Nx has $H_{\text{smx}}^2 = (8\pi G/3)\rho_{\text{smx}}$ with $\rho_{\text{smx}} \equiv \rho_r^{\text{smx}} + \rho_m^{\text{smx}} + \rho_\Lambda^{\text{smx}}$. For simplicity we assume

the same amount of matter in both models and we take for model ρ^{smx} the following content:

- (i) for $a \leq a_c$ we have extra radiation $\rho_{\text{ex}} \neq 0$ with $\rho_r^{\text{smx}} = \rho_r^{\text{sm}} + \rho_{\text{ex}}$ and $\rho_m^{\text{smx}} = \rho_m^{\text{sm}}$;
- (ii) for $a > a_c$, we have $\rho_{\text{ex}} = 0$, $\rho_r^{\text{smx}} = \rho_r^{\text{sm}}$, $\rho_m^{\text{smx}} = \rho_m^{\text{sm}}$ but $\rho_\Lambda^{\text{smx}} > \rho_\Lambda^{\text{sm}}$.

We will now determine the relation between the amount $\rho_{\text{ex}}(a_c)$ [or, equivalently, $\Omega_{\text{ex}}(a_c)$] as a function of the transition scale a_c such that the ratio of the sound horizon $r_s(a_*)$ at decoupling and the angular distance to the last scattering surface $D_A(a_*)$ is unchanged, thus preserving the acoustic angle $\theta(a_*)$ as measured by *Planck* [4], but with a Hubble parameter H_0 in the $\Lambda\text{CDM-Nx}$ (“smx”) model consistent with the high value of local measurements $H_0^R = 74$ [4]. Taking $H_0^{\text{sm}} = H_0^P = 67$ and $H_0^{\text{smx}} = H_0^R = 74$, the ratio $D_A^{\text{smx}}(a_*)/D_A^{\text{sm}}(a_*)$ gives

$$\xi = D_A^{\text{smx}}(a_*)/D_A^{\text{sm}}(a_*) = 0.981. \quad (7)$$

Since $\xi < 1$ and using Eq. (6), we require $r_s^{\text{smx}}(a_*)/r_s^{\text{sm}}(a_*)$ to be smaller than one. We can achieve this by increasing $H(a)$ in the region $a \leq a_*$ in $\Lambda\text{CDM-Nx}$ compared to the standard ΛCDM model by introducing extra radiation $\rho_{\text{ex}}(a)$ in the region $a < a_*$. With this modification, we tune $\rho_{\text{ex}}(a_c)$ to obtain the ratio $r_s^{\text{smx}}(a_*)/r_s^{\text{sm}}(a_*)$ in order to obtain the same value of $\theta(a_*)$ in Eq. (6) as measured by *Planck* 2018.

Let us compare the Hubble parameter in these two models in the region $a \ll a_o$, where dark energy is subdominant, which gives

$$\frac{H_{\text{sm}}}{H_{\text{smx}}} = \sqrt{\frac{\rho_r^{\text{sm}} + \rho_m^{\text{sm}}}{\rho_r^{\text{sm}} + \rho_m^{\text{sm}} + \rho_{\text{ex}}}} = \sqrt{1 - \Omega_{\text{ex}}}, \quad (8)$$

with

$$\Omega_{\text{ex}} \equiv \frac{\rho_{\text{ex}}}{\rho_{\text{smx}}} = \frac{\rho_{\text{ex}}}{\rho_{\text{sm}} + \rho_{\text{ex}}} \simeq \frac{N_{\text{ex}}\beta}{1 + (N_\nu + N_{\text{ex}})\beta}, \quad (9)$$

where the last term in Eq. (9) is given in terms of relativistic degrees of freedom with $\rho_{\text{sm}} = g_{\text{sm}}\rho_\gamma$, $\rho_{\text{ex}} = g_{\text{ex}}\rho_\gamma$, and $g_{\text{sm}} = 1 + N_\nu\beta$, $g_{\text{ex}} = N_{\text{ex}}\beta$, $g_{\text{smx}} = g_{\text{sm}} + g_{\text{ex}}$ with $\rho_\gamma = \frac{\pi^2}{30}g_\gamma T_\gamma^4$, $N_\nu = 3.046$, and where N_{ex} is the number of the extra-relativistic degrees of freedom in terms of the neutrino temperature and $\beta = (7/8)(4/11)^{4/3}$. Notice that the last approximation in Eq. (9) is only valid in the radiation-dominated epoch. Since we assume in our models ΛCDM and $\Lambda\text{CDM-Nx}$ the same amount of matter and radiation at present time but different values of H_0 , we must necessarily have a larger amount of dark energy in model $\Lambda\text{CDM-Nx}$ than in ΛCDM to account for the increase value in H_0 . We constrain the $\Lambda\text{CDM-Nx}$ model by imposing that it gives the same acoustic angle $\theta(a_*) = r_s(a_*)/D_A(a_*)$ as

ΛCDM [cf. Eq. (5)] and a relative quotient of $r_s(a_*)$ and $D_A(a_*)$ as in Eq. (6).

We will now compare the Hubble parameter H in the ΛCDM (sm) and $\Lambda\text{CDM-Nx}$ (smx) models. By our working hypothesis, both models have the same amount of matter and radiation at present time, while the value of H_0 differs with $H_0^P = 67$ for ΛCDM (sm) and $H_0^R = 73$ for $\Lambda\text{CDM-Nx}$ (smx). Let us express H as

$$H^{\text{sm}}(a) = H_0^{\text{sm}} \sqrt{\Omega_{mo}^{\text{sm}}(a/a_o)^{-3} + \Omega_{ro}^{\text{sm}}(a/a_o)^{-4} + \Omega_{\Lambda o}^{\text{sm}}} \quad (10)$$

and

$$H^{\text{smx}}(a) = H_0^{\text{smx}} \sqrt{\Omega_{mo}^{\text{smx}}(a/a_o)^{-3} + \Omega_{ro}^{\text{smx}}(a/a_o)^{-4} + \Omega_{\Lambda o}^{\text{smx}}} \quad (11)$$

with the constraint $\Omega_{mo} + \Omega_{ro} + \Omega_{\Lambda o} = 1$ for both models. Since by assumption we have the same amount of matter and radiation, $\rho_{mo}^{\text{sm}} = \rho_{mo}^{\text{smx}}$ and $\rho_{ro}^{\text{sm}} = \rho_{ro}^{\text{smx}}$, we simply multiply and divide by the critical density ρ_{co} of each model to get

$$\rho_{qo} = \Omega_{qo}^{\text{sm}} \rho_{co}^{\text{sm}} = \Omega_{qo}^{\text{smx}} \rho_{co}^{\text{smx}}, \quad (12)$$

$$\rho_{\Lambda o}^{\text{smx}} = \rho_{\Lambda o}^{\text{sm}} + \rho_{co}^{\text{sm}} \left(\frac{(H_0^{\text{smx}})^2}{(H_0^{\text{sm}})^2} - 1 \right), \quad (13)$$

with $q = m, r$ for matter and radiation, respectively. ΛCDM (sm) and $\Lambda\text{CDM-Nx}$ (smx) have the same ρ_{mo} and ρ_{ro} , but a different value for H_0 gives a different amount of dark energy ρ_Λ , as seen in Eq. (13). We clearly see in Eq. (13) how different values of H_0 impact the dark energy density in these two models. We further express

$$\Omega_{qo}^{\text{smx}} = \frac{(H_0^{\text{sm}})^2}{(H_0^{\text{smx}})^2} \Omega_{qo}^{\text{sm}},$$

$$\Omega_{\Lambda o}^{\text{smx}} = 1 - (\Omega_{mo}^{\text{smx}} + \Omega_{ro}^{\text{smx}}) = 1 - \frac{(H_0^{\text{sm}})^2}{(H_0^{\text{smx}})^2} (\Omega_{mo}^{\text{sm}} + \Omega_{ro}^{\text{sm}}). \quad (14)$$

The Hubble parameter H becomes

$$H^s(a) = H_0^s \sqrt{1 + \Omega_{mo}^s [(a/a_o)^{-3} - 1] + \Omega_{ro}^s [(a/a_o)^{-4} - 1]}, \quad (15)$$

with $s = \text{sm}$ and smx for the ΛCDM and $\Lambda\text{CDM-Nx}$ models, respectively. Expressing H^{smx} in terms of standard model “sm” quantities we have for “smx” model a Hubble parameter $H^{\text{smx}}(a)$ given by

$$H^{\text{smx}} = H_0^{\text{smx}} \sqrt{1 + (H_0^{\text{sm}}/H_0^{\text{smx}})^2 F(a)} \quad (16)$$

$$= H_0^{\text{sm}} \sqrt{(H_0^{\text{smx}}/H_0^{\text{sm}})^2 + F(a)}, \quad (17)$$

with $F(a) \equiv \Omega_{mo}^{\text{sm}}[(a/a_o)^{-3} - 1] + \Omega_{ro}^{\text{sm}}[(a/a_o)^{-4} - 1]$.

We have expressed $H^{\text{smx}}(a)$ in terms of quantities of the model sm and the ratio $H_0^{\text{sm}}/H_0^{\text{smx}}$. The difference in H^{sm} in ΛCDM and H^{smx} in $\Lambda\text{CDM-Nx}$ due to the distinct values of H_0 is manifested in the first terms in the square root in Eqs. (15) and (17) [1 in Eq. (15) compared to $(H_0^{\text{smx}}/H_0^{\text{sm}})^2$ in Eq. (17)], with $(H_0^{\text{smx}}/H_0^{\text{sm}})^2 = (H_0^R/H_0^P)^2 = (74/67)^2 = 1.22$ for our two fiducial examples.

B. Impact of ρ_{ex} on the acoustic scale $r_s(a_*)$

We will now quantify the impact on the acoustic scale $r_s(a_*)$ from having extra-relativistic energy density $\rho_{\text{ex}}(a)$, present before recombination, helps to conciliate the H_0 tension between early and late-time measurements. We assume that ρ_{ex} is present up to the scale factor a_c and that it dilutes rapidly [66] and no longer contributes to H . The rapid dilution of ρ_{ex} can be motivated by a BDE model [62,63] or EDE models [22,24]. Interestingly, an extra energy density ρ_{ex} , with a rapid energy density dilution at a_c , besides contributing towards a solution to the H_0 crisis, may also leave interesting signatures in the matter power spectrum [61,63,65,66,72], so we may correlate the H_0 solution with cluster counts.

Let us now study the impact of ρ_{ex} on the H_0 tension problem and its cosmological signatures. From Eq. (8), we take $H_{\text{sm}}/H_{\text{smx}} = \sqrt{1 - \Omega_{\text{ex}}}$, and for simplicity and presentation purposes we consider that Ω_{ex} is constant for $a \leq a_c$ and $\Omega_{\text{ex}} = 0$, and $H_{\text{smx}} = H_{\text{sm}}$ for $a > a_c$. The precise impact of Ω_{ex} and the value of a_c on the different cosmological parameters must be numerically calculated. We implement $\Lambda\text{CDM-Nx}$ in a Boltzmann code and run Markov chains (we use CAMB and COSMOMC [67–71]), and we present the results in Sec. IV.

Nevertheless, having approximate analytic expressions of the acoustic scale allows us to have a simple grasp of the impact of ρ_{ex} and a_c on the magnitude of $r_s(a_*)$ and a possible solution to the H_0 crisis. The change in the acoustic scale $r_s(a_*)$ in ΛCDM (sm) and $\Lambda\text{CDM-Nx}$ (smx) can be easily estimated. Let us consider the difference

$$\begin{aligned} r_s^{\text{sm}}(a_*) - r_s^{\text{smx}}(a_*) &= \int_{a_i}^{a_*} \frac{c_s da}{a^2 H_{\text{sm}}} - \int_{a_i}^{a_*} \frac{c_s da}{a^2 H_{\text{smx}}} \\ &= \int_{a_i}^{a_c} \frac{c_s da}{a^2 H_{\text{sm}}} - \int_{a_i}^{a_c} \frac{c_s da}{a^2 H_{\text{smx}}} \\ &\equiv r_s^{\text{sm}}(a_c) - r_s^{\text{smx}}(a_c), \end{aligned} \quad (18)$$

where we have taken into account that $H_{\text{smx}} = H_{\text{sm}}$ for $a > a_c$ and the integrals from $a_c \leq a \leq a_*$ cancel out. As

long as $H_{\text{sm}}/H_{\text{smx}} = \sqrt{1 - \Omega_{\text{ex}}}$ is constant, we can simply write

$$\begin{aligned} r_s^{\text{smx}}(a_c) &\equiv \int_{a_i}^{a_c} \frac{c_s da}{a^2 H_{\text{smx}}} = \int_{a_i}^{a_c} \left(\frac{H_{\text{sm}}}{H_{\text{smx}}} \right) \frac{c_s da}{a^2 H_{\text{sm}}} \\ &= \sqrt{1 - \Omega_{\text{ex}}} r_s^{\text{sm}}(a_c). \end{aligned} \quad (19)$$

Clearly, the value of Ω_{ex} determines the ratio of $r_s^{\text{smx}}(a_*)/r_s^{\text{sm}}(a_*)$. Now, by writing $r_s^{\text{sm}}(a_*) - r_s^{\text{smx}}(a_*) = r_s^{\text{sm}}(a_*)(1 - \xi)$ with ξ given in Eq. (6) and $r_s^{\text{sm}}(a_c) - r_s^{\text{smx}}(a_c) = r_s^{\text{sm}}(a_c)(1 - \sqrt{1 - \Omega_{\text{ex}}})$ from Eq. (18), we obtain $r_s^{\text{sm}}(a_*)(1 - \xi) = r_s^{\text{sm}}(a_c)(1 - \sqrt{1 - \Omega_{\text{ex}}})$ and

$$\frac{r_s^{\text{sm}}(a_*)}{r_s^{\text{sm}}(a_c)} = \frac{1 - \sqrt{1 - \Omega_{\text{ex}}}}{1 - \xi}. \quad (20)$$

If we assume radiation domination, the quantity $a^2 H$ is constant, and by also taking c_s to be constant (for simplicity and presentation purposes) we get

$$\frac{r_s^{\text{sm}}(a_*)}{r_s^{\text{sm}}(a_c)} = \frac{\int_{a_i}^{a_*} \frac{da c_s}{a^2 H_{\text{sm}}}}{\int_{a_i}^{a_c} \frac{da c_s}{a^2 H_{\text{sm}}}} = \frac{a_c H_{\text{sm}}(a_c)}{a_* H_{\text{sm}}(a_*)} = \frac{a_*}{a_c}, \quad (21)$$

and Eq. (20) becomes

$$\left(\frac{a_*}{a_c} \right) = \frac{1 - \sqrt{1 - \Omega_{\text{ex}}}}{1 - \xi} = 52.63(1 - \sqrt{1 - \Omega_{\text{ex}}}), \quad (22)$$

where we have set $\xi = 0.981$ [our fiducial value in Eq. (6)]. Equation (22) gives a very simple analytic solution for a_c as a function of Ω_{ex} with the constraint that we have the same acoustic angle $\theta(a_*)$ [cf. Eq. (1)] in $\Lambda\text{CDM-Nx}$ with $H_0 = 74$ as in the ΛCDM model with $H_0 = 67$. We see in Eq. (22) that larger values of a_c require smaller values of Ω_{ex} . In Fig. 1 we plot the required values of N_{ex} and Ω_{ex} as functions of $x = a_c/a_{\text{eq}}$ using Eq. (22) and from the numerical calculation solving the full $H(a)$ as given in Eqs. (10) and (11). We should keep in mind that Eq. (22) is only an approximation since we assumed radiation domination; however, it gives a simple estimation of the required value of Ω_{ex} required to obtain the size of the acoustic scale determined by *Planck* data [P18] and the value of H_0 measured by Riess et al [R19].

C. Matter power spectrum and ρ_{ex}

We have seen in the previous section how ρ_{ex} impacts cosmological distances and contributes to reducing the H_0 tension. The rapid dilution of ρ_{ex} affects the evolution of density perturbations and the matter power spectrum $P(k, z)$ [25,33,43,44,57,58,61,66]. Interestingly, an energy density $\rho_{\text{ex}}(a)$ that dilutes rapidly at $a = a_c$ (see Sec. III B) will leave detectable imprints on the matter power spectrum, which can be correlated with a possible solution to the H_0 tension. We can estimate the location and

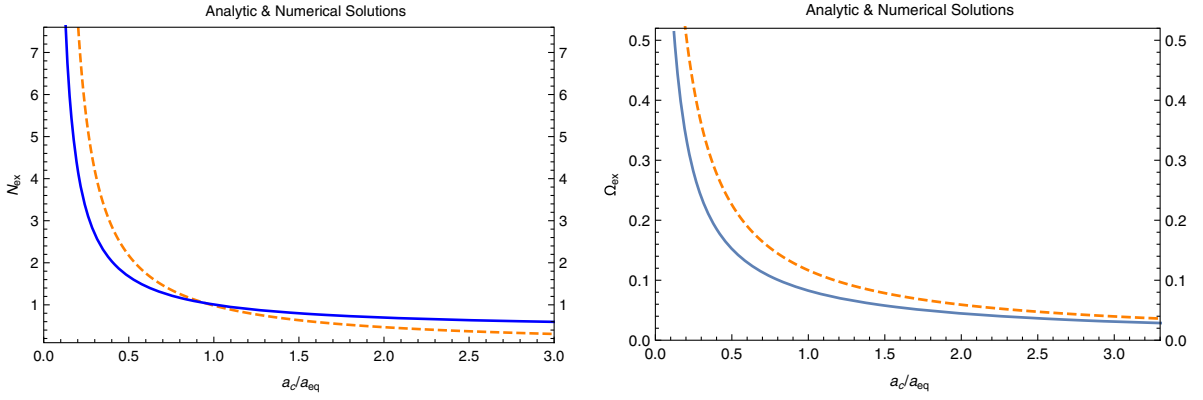


FIG. 1. Analytic and numerical solutions for $N_{\text{ex}}(a_c)$ and $\Omega_{\text{ex}}(a_c)$. We plot N_{ex} (left panel) and Ω_{ex} (right panel) as functions of $x \equiv a_c/a_{\text{eq}}$ satisfying the constraint $r_s^{\text{smx}}(a_*)/r_s^{\text{sm}}(a) = \xi$ [cf. Eq. (7)]. We plot the numerical solution (blue) using Eq. (3) and the analytic solution (dashed-orange) using Eq. (22).

magnitude of this bump produced at the transition scale a_c corresponding to the mode

$$k_c \equiv a_c H_c, \quad (23)$$

with $H_c \equiv H(a_c)^2 = (8\pi G/3)\rho_{\text{smx}}(a_c)$ and $\rho_{\text{smx}} = \rho_{\text{sm}} + \rho_{\text{ex}}$. The amplitude of the bump is related to the magnitude of $\rho_{\text{ex}}(a)$, while the width of the bump is related to how fast ρ_{ex} dilutes [66]. During radiation domination the amplitude $\delta_m = \delta\rho_m/\rho_m$ has a logarithmic growth,

$$\delta_m^{\text{smx}}(a) = \delta_{mi}^{\text{smx}}(\ln(a/a_h^{\text{smx}}) + 1/2), \quad (24)$$

$$\delta_m^{\text{sm}}(a) = \delta_{mi}^{\text{sm}}(\ln(a/a_h^{\text{sm}}) + 1/2), \quad (25)$$

where a_h corresponds to the horizon crossing. Comparing the growth of δ_m for the same mode in both cases $k^{\text{smx}} = k^{\text{sm}}$ with $k^{\text{sm}} = a_h^{\text{sm}} H^{\text{sm}}(a_h^{\text{sm}})$ and $k^{\text{smx}} = a_h^{\text{smx}} H^{\text{smx}}(a_h^{\text{smx}})$. Modes $k > k_c$ cross the horizon at $a_h < a_c$ and we find from Eq. (8) that

$$\frac{a_h^{\text{smx}}}{a_h^{\text{sm}}} = \frac{H^{\text{sm}}}{H^{\text{smx}}} = \sqrt{1 - \Omega_{\text{ex}}}. \quad (26)$$

The ratio $\Delta\delta_m = \delta_m^{\text{smx}}/\delta_m^{\text{sm}} = (\delta_{mi}^{\text{smx}}/\delta_{mi}^{\text{sm}})(\ln(a/a_h^{\text{smx}}) + 1/2)/(\ln(a/a_h^{\text{sm}}) + 1/2)$ can be expressed for $a > a_c$ as

$$\Delta\delta_m = \frac{\delta_{mi}^{\text{smx}}}{\delta_{mi}^{\text{sm}}} \frac{\left[\left(\frac{H_+^{\text{smx}}}{H_-^{\text{smx}}} \right) \ln\left(\frac{a}{a_c}\right) + \ln\left(\frac{a_h^{\text{sm}}}{a_h^{\text{smx}}}\right) + \ln\left(\frac{a_c}{a_h^{\text{sm}}}\right) + \frac{1}{2} \right]}{\ln\left(\frac{a}{a_c}\right) + \ln\left(\frac{a_c}{a_h^{\text{sm}}}\right) + \frac{1}{2}}, \quad (27)$$

where $H_+^{\text{smx}}(a_c)$ contains ρ_{ex} and $H_-^{\text{smx}}(a_c)$ has $\rho_{\text{ex}} = 0$. For presentation purposes, here we have consider a step function at a_c with $\rho_{\text{ex}}(a) = 0$ for $a < a_c$, and we have $H_+^{\text{smx}}(a_c)/H_-^{\text{smx}}(a_c) = H^{\text{smx}}(a_c)/H^{\text{sm}}(a_c) = 1/\sqrt{1 - \Omega_{\text{ex}}}$. Equation (27)

is valid for modes $k > k_c$ entering the horizon at $a_h < a_c$. The increase for modes $k > k_c$ at present time is

$$\Delta\delta_m = \frac{\delta_m^{\text{smx}}}{\delta_m^{\text{sm}}} = \frac{\delta_{mi}^{\text{smx}}}{\delta_{mi}^{\text{sm}}} \frac{H_+^{\text{smx}}}{H_-^{\text{sm}}} = \frac{\delta_{mi}^{\text{smx}}}{\delta_{mi}^{\text{sm}}} \frac{1}{\sqrt{1 - \Omega_{\text{ex}}}}, \quad (28)$$

where we assumed that $a_o \gg a_c$. On the other hand, modes $k < k_c$ do not undergo the transition and are not boosted by the rapid dilution of ρ_{ex} . The final result in the matter power spectrum is the generation of a bump in the ratio $P_{\text{smx}}/P_{\text{sm}}$ at scales of the order of k_c .

To conclude, we have seen in our toy model that an extra-relativistic energy density ρ_{ex} may alleviate the tension in the H_0 measurements and at the same time leave detectable signals in the matter power spectrum, allowing for a verification of the proposal.

IV. COSMOLOGICAL RESULTS AND MCMC IMPLEMENTATION

Here we consider two models: the first model is simply the standard Λ CDM model, while our second model corresponds to an extension to Λ CDM, where we add extra-relativistic energy density $\rho_{\text{ex}}(a) \propto 1/a^3$ present only at early times for a scale factor a smaller than a_c , corresponding to the transition scale factor, and the extra energy density dilutes as $\rho_{\text{ex}} \propto a^{-6}$ for $a \gg a_c$ and therefore rapidly becomes negligible. We refer to this latter model as Λ CDM-Nx and it is motivated by the BDE model [62,63] and EDE models [42–45].

With this rapid dilution we avoid a step function transition at a_c in the evolution of $\rho_{\text{ex}}(a)$. Clearly, ρ_{ex} dilutes faster than radiation for $a > a_c$ and its contribution rapidly becomes subdominant. The energy density ρ_{ex} can also be parametrized by the number of extra-relativistic degrees of freedom N_{ex} , defined in terms of the neutrino temperature T_ν as $\rho_{\text{ex}} = (\pi^2/30)N_{\text{ex}}T_\nu^4$. We implement the Λ CDM-Nx model in the Boltzmann code CAMB [67–71] and perform a full COSMOMC analysis for Λ CDM and

TABLE I. We show the best-fit, marginalized, and 68% confidence limits on cosmological parameters for Λ CDM-Nx and Λ CDM with *Planck* 2018 TT,TE,EE-lowE and local H_0 R19 measurements and Λ CDM without R19 (i.e., “No-Riess”).

Model parameter	Λ CDM-Nx $H_0 = (74.03 \pm 1.42)$		Λ CDM $H_0 = 74.03 \pm 1.42$		Λ CDM H_0 no-riess	
	Best-fit sampling		Best-fit sampling		Best-fit sampling	
a_c	0.00071	$0.407^{+0.105}_{-0.241} \times 10^{-6}$
$\Omega_{\text{ex}}(a_c)$	0.00353	$0.063^{+0.146}_{-0.021}$
N_{ex}	0.09034	$0.81^{+0.22}_{-0.79}$
H_0	69.14	68.70 ± 0.45	68.557	68.54 ± 0.43	67.961	67.99 ± 0.45
Ω_Λ	0.702	0.7007 ± 0.0057	0.700	0.6997 ± 0.0056	0.692	0.6925 ± 0.0060
Ω_m	0.298	0.2993 ± 0.0057	0.300	0.3003 ± 0.0056	0.308	0.3075 ± 0.0060
$\Omega_m h^2$	0.142	0.14123 ± 0.00093	0.141	0.14106 ± 0.00092	0.142	0.14209 ± 0.00096
$\Omega_b h^2$	0.022	0.02257 ± 0.00014	0.022	0.02248 ± 0.00013	0.022	0.02237 ± 0.00013
z_{eq}	3398.84	3375 ± 22	3370.15	3371 ± 22	3397.99	3396 ± 23
$\ln(10^{10} A_s)$	3.048	3.049 ± 0.017	3.047	3.046 ± 0.017	3.044	3.045 ± 0.016
n_s	0.973	$0.9722^{+0.0043}_{-0.0049}$	0.970	0.9683 ± 0.0037	0.966	0.9655 ± 0.0038
σ_8	0.826	0.8237 ± 0.0079	0.821	0.8206 ± 0.0075	0.824	0.8235 ± 0.0072
S_8	0.823	0.823 ± 0.013	0.821	0.821 ± 0.012	0.835	0.834 ± 0.013
z_{drag}	1089.81	$1060.63^{+0.38}_{-0.56}$	1060.12	1060.09 ± 0.28	1059.93	1059.92 ± 0.28
r_{drag}	146.60	101.11 ± 0.76	147.35	147.35 ± 0.24	147.14	147.17 ± 0.24
z_\star	1060.24	$1089.95^{+0.26}_{-0.35}$	1089.63	1089.65 ± 0.21	1089.88	1089.88 ± 0.22
r_\star	143.98	144.58 ± 0.25	144.72	144.72 ± 0.23	144.48	144.51 ± 0.24
$D_A(r_\star)/\text{Gpc}$	13.829	13.885 ± 0.024	13.899	13.898 ± 0.022	13.877	13.880 ± 0.023
$100\theta(z_\star)$	1.0410	1.04137 ± 0.00036	1.0411	1.04115 ± 0.00029	1.0410	1.04099 ± 0.00029
$\chi^2_{H_0}$	11.84	14.2 ± 2.4	14.854	15.0 ± 2.4
χ^2_{CMB}	2766.24	2782.6 ± 6.1	2765.69	2781.3 ± 5.8	2764.35	2780.0 ± 5.7

Λ CDM-Nx for several data sets, and we present the results and conclusions in Sec. IV A.

Since our main interest here is to study the tension between the inferred value of H_0 from early CMB physics and late-time local measurements of H_0 , we use the CMB (TT, TE, EE + lowE) data set from *Planck* 2018 [P18] and the recent measurements from SHOES, $H_0^R = (74.03 \pm 1.42)$ at the 68% confidence level, from [R19]. We run Markov chain Monte Carlo (MCMC) simulations for both models— Λ CDM and Λ CDM-Nx—and compare the posterior probabilities, and we assess the viability to alleviate the H_0 tension between CMB data from *Planck* [P18] and local H_0 measurements [R19]. We decided not to use BAO measurements, keeping in mind that BAO is consistent with high and low values of H_0 and it is in the context of Λ CDM that BAO measurements hint at a lower value of H_0 [60]. Besides, BAO analysis is strongly impacted by the late-time dynamics of dark energy at low redshifts $z < 5$. Changes in BAO analysis due to a dynamical dark energy are beyond the scope in this work since we want to concentrate here on the tension between CMB and local H_0 measurements.

For our analysis we consider—in addition to the recent measurement $H_0^R = 74.03 \pm \sigma_H$ with $\sigma_H = 1.42$ at the 68% confidence level (we will quote all values of H_0 and σ_H in units of $\text{km s}^{-1} \text{Mpc}^{-1}$)—two forecasting values of σ_H and we take these forecasting values as $\sigma_H = 1$ and

$\sigma_H = 0.5$. With these two forecasting values of σ_H we impose a “tighter observational” constraint on H_0 from local measurements to study the impact on the posterior probabilities of H_0 and other relevant cosmological parameters in the Λ CDM and Λ CDM-Nx models, and we assess the price we have to pay regarding the “goodness of fit” of CMB, χ^2_{CMB} , for these two forecasting values of H_0 . Notice, however, that these forecasting values, $\sigma_H = 1$ and $\sigma_H = 0.5$, are of the same order of magnitude as the average value obtained in Ref. [14] with an average value of local measurements of $H_0 = (73.03 \pm 0.8) \text{ km s}^{-1} \text{Mpc}^{-1}$.

We first consider the MCMC results using CMB data [P18] and $H_0 = (74.02 \pm \sigma_H)$ with $\sigma_H = 1.42$ [R19]. We show the best-fit and marginalized values at the 68% confidence level for Λ CDM-Nx and Λ CDM for different cosmological parameters in Table I. For completeness, we also include Λ CDM without the Riess H_0 data set (we refer to this case as “No-Riess”). Notice that the value of H_0 in Table I is slightly increased from $H_0 = (67.99 \pm 0.45)$ in Λ CDM without the Riess data [R19] to $H_0 = (68.54 \pm 0.43)$ for Λ CDM and a value of $H_0 = (68.70 \pm 0.45)$ in Λ CDM-Nx where we included Riess data [R19] in these last two cases. The values of H_0 correspond to mild increases of 0.81% and 1.04%, in the value of H_0 for Λ CDM and Λ CDM-Nx, respectively. These values of H_0 are still in disagreement with local measurements

TABLE II. Best-fit, marginalized, and 68% confidence limits for Λ CDM with *Planck* 2018 TT,TE,EE-lowE data and $H_0 = 74.02 \pm \sigma_H$ with the forecasting values $\sigma_H = 1$ and $\sigma_H = 0.5$

Model parameter	Λ CDM $H_0 = 74.03 \pm 1$		Λ CDM $H_0 = 74.03 \pm 0.5$	
	Best-fit sampling		Best-fit sampling	
H_0	69.050	69.04 ± 0.41	70.789	70.79 ± 0.36
Ω_Λ	0.706	0.7059 ± 0.0052	0.727	0.7268 ± 0.0041
Ω_m	0.294	0.2941 ± 0.0052	0.273	0.2732 ± 0.0041
$\Omega_m h^2$	0.140	0.14013 ± 0.00089	0.137	0.13690 ± 0.00077
$\Omega_b h^2$	0.023	0.02258 ± 0.00013	0.023	0.02291 ± 0.00013
z_{eq}	3349.60	3349 ± 21	3272.72	3272 ± 18
$\ln(10^{10} A_s)$	3.046	3.046 ± 0.017	3.049	$3.051^{+0.017}_{-0.019}$
n_s	0.972	0.9712 ± 0.0036	0.981	0.9805 ± 0.0036
σ_8	0.818	0.8180 ± 0.0074	0.808	$0.8089^{+0.0072}_{-0.0082}$
S_8	0.810	0.810 ± 0.012	0.772	0.772 ± 0.011
z_{drag}	1060.31	1060.24 ± 0.27	1060.77	1060.73 ± 0.28
r_{drag}	147.48	147.51 ± 0.24	148.08	148.11 ± 0.23
z_\star	1089.41	1089.44 ± 0.20	1088.72	1088.74 ± 0.18
r_\star	144.89	144.91 ± 0.23	145.58	145.60 ± 0.21
$D_A(r_\star)/\text{Gpc}$	13.913	13.915 ± 0.022	13.973	13.974 ± 0.021
$100\theta(z_\star)$	1.0413	1.04128 ± 0.00029	1.0418	1.04178 ± 0.00028
$\chi^2_{H_0}$	24.797	25 ± 4	42.027	42 ± 9
χ^2_{CMB}	2766.43	2782.1 ± 6.2	2784.45	2800.3 ± 7.8

[R19]. The model Λ CDM-Nx contains extra radiation, $\Omega_{\text{ex}}(a_c) = 0.063(+0.146, -0.021)$, with $N_{\text{ex}} = 0.0903(+0.28, -0.79)$ at the 68% confidence level.

We follow up our analysis by considering $H_0^R = (74.03 \pm \sigma_H)$ with the two forecasting values $\sigma_H = 1$ and $\sigma_H = 0.5$. With these forecasting values for σ_H , we

TABLE III. Best-fit, marginalized, and 68% confidence limits for Λ CDM-Nx with *Planck* 2018 TT,TE,EE-lowE data and $H_0 = 74.02 \pm \sigma_H$ with the forecasting values $\sigma_H = 1$ and $\sigma_H = 0.5$.

Model parameter	Λ CDM-Nx $H_0 = 74.03 \pm 1$		Λ CDM-Nx $H_0 = 74.03 \pm 0.5$	
	Best-fit sampling		Best-fit sampling	
a_c	0.00015	$0.407^{+0.105}_{-0.245} \times 10^{-6}$	0.00348	$4.898^{+2.247}_{-2.710} \times 10^{-3}$
$\Omega_{\text{ex}}(a_c)$	0.00623	$0.079^{+0.161}_{-0.023}$	0.00603	$4.786^{+5.447}_{-1.319} \times 10^{-3}$
N_{ex}	0.07059	$0.99^{+0.28}_{-0.95}$	0.60916	0.69 ± 0.10
H_0	69.23	69.19 ± 0.44	72.83	72.99 ± 0.47
Ω_Λ	0.705	0.7067 ± 0.0053	0.718	0.7151 ± 0.0045
Ω_m	0.2949	0.2933 ± 0.0053	0.2825	0.2849 ± 0.0045
$\Omega_m h^2$	0.1413	0.14039 ± 0.00090	0.1499	0.1518 ± 0.0024
$\Omega_b h^2$	0.0227	0.02267 ± 0.00015	0.0230	0.02300 ± 0.00012
z_{eq}	3377.26	3355 ± 22	3581.23	3628 ± 59
$\ln(10^{10} A_s)$	3.0502	3.051 ± 0.017	3.0699	$3.076^{+0.016}_{-0.018}$
n_s	0.9776	$0.9753^{+0.0046}_{-0.0052}$	0.9911	0.9917 ± 0.0040
σ_8	0.8258	0.8220 ± 0.0080	0.8472	0.854 ± 0.010
S_8	0.8187	0.813 ± 0.012	0.8221	0.832 ± 0.014
z_{drag}	1060.58	$1060.87^{+0.43}_{-0.61}$	1062.30	1062.51 ± 0.38
r_{drag}	146.92	147.31 ± 0.28	141.80	141.0 ± 1.0
z_\star	1089.45	$1089.83^{+0.28}_{-0.36}$	1090.31	1090.53 ± 0.32
r_\star	144.36	144.74 ± 0.26	139.40	138.6 ± 1.0
$D_A(r_\star)$	13.860	13.899 ± 0.024	13.404	13.330 ± 0.095
$100\theta(z_\star)$	1.0414	1.04155 ± 0.00038	1.0403	1.04013 ± 0.00036
$\chi^2_{H_0}$	23.031	24 ± 4	5.71714	5.2 ± 4.2
χ^2_{CMB}	2767.06	2784.9 ± 6.4	2779.81	2797.9 ± 6.9

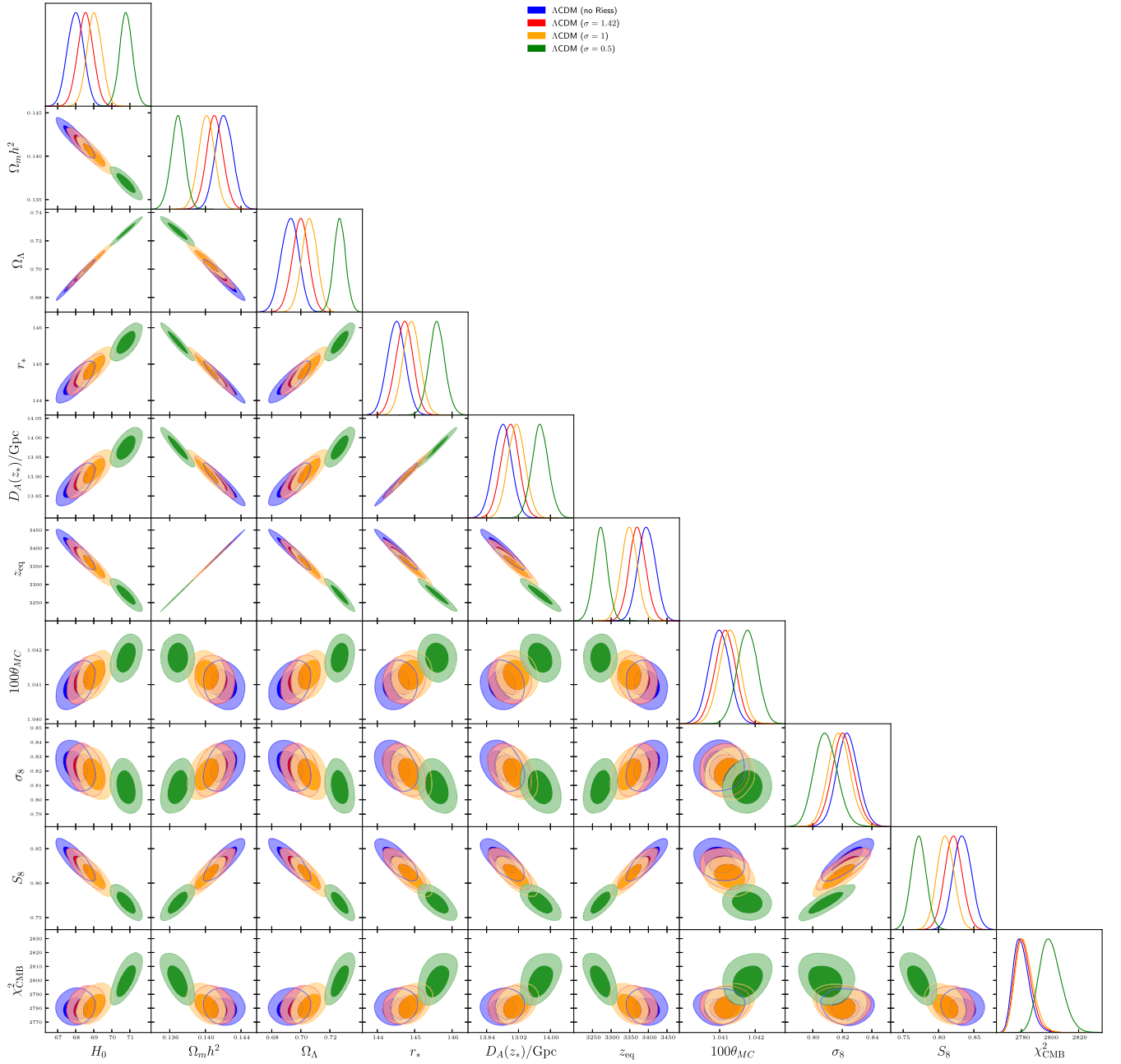


FIG. 2. Marginalized 68% and 95% parameter constraint contours for Λ CDM using *Planck* 2018 TT,TE,EE,lowE data [P18] and $H_0 = (74.03 \pm \sigma_H) \text{ km s}^{-1} \text{ Mpc}^{-1}$ with $\sigma_H = 1.42$ [R19], the forecasting values $\sigma_H = 1, 0.5$, and Λ CDM without the Riess data set.

impose a tighter constraint on the value of H_0 and this allows to assess the impact on the posterior probabilities of the cosmological parameters as well as the goodness fit for CMB, χ^2_{CMB} . We implement these forecasting values ($\sigma_H = 1$ and $\sigma_H = 0.5$) in the MCMC analysis for the Λ CDM and Λ CDM-Nx models. We show the best-fit values and posterior probabilities at 68% C.L. in Table II for Λ CDM and in Table III for Λ CDM-Nx. For the Λ CDM model with the forecasting value $\sigma_H = 1$ we find a value of $H_0 = 69.04 \pm 0.41$ (68% C.L.) and a best-fit value $H_0 = 69.05$, while for $\sigma_H = 0.5$ we find

$H_0 = 70.79 \pm 0.36$ (68% C.L.) and $H_0 = 70.79$ for the best fit. In the Λ CDM-Nx model we obtain for $\sigma_H = 1$ a value $H_0 = 69.19 \pm 0.44$ with a best fit $H_0 = 69.23$, and for $\sigma_H = 0.5$ we get $H_0 = 72.99 \pm 0.47$ and a best fit 72.83 . We notice that a reduced $\sigma_H = 0.5$ substantially increases the value of H_0 in Λ CDM-Nx but not in Λ CDM. This is no surprise and is a consequence of the contribution of the extra-relativistic energy density ρ_{ex} in Λ CDM-Nx.

We present the best-fit values and marginalized 68% and 95% parameter constraint contours for different cosmological parameters for Λ CDM in Fig. 2 and for Λ CDM-Nx

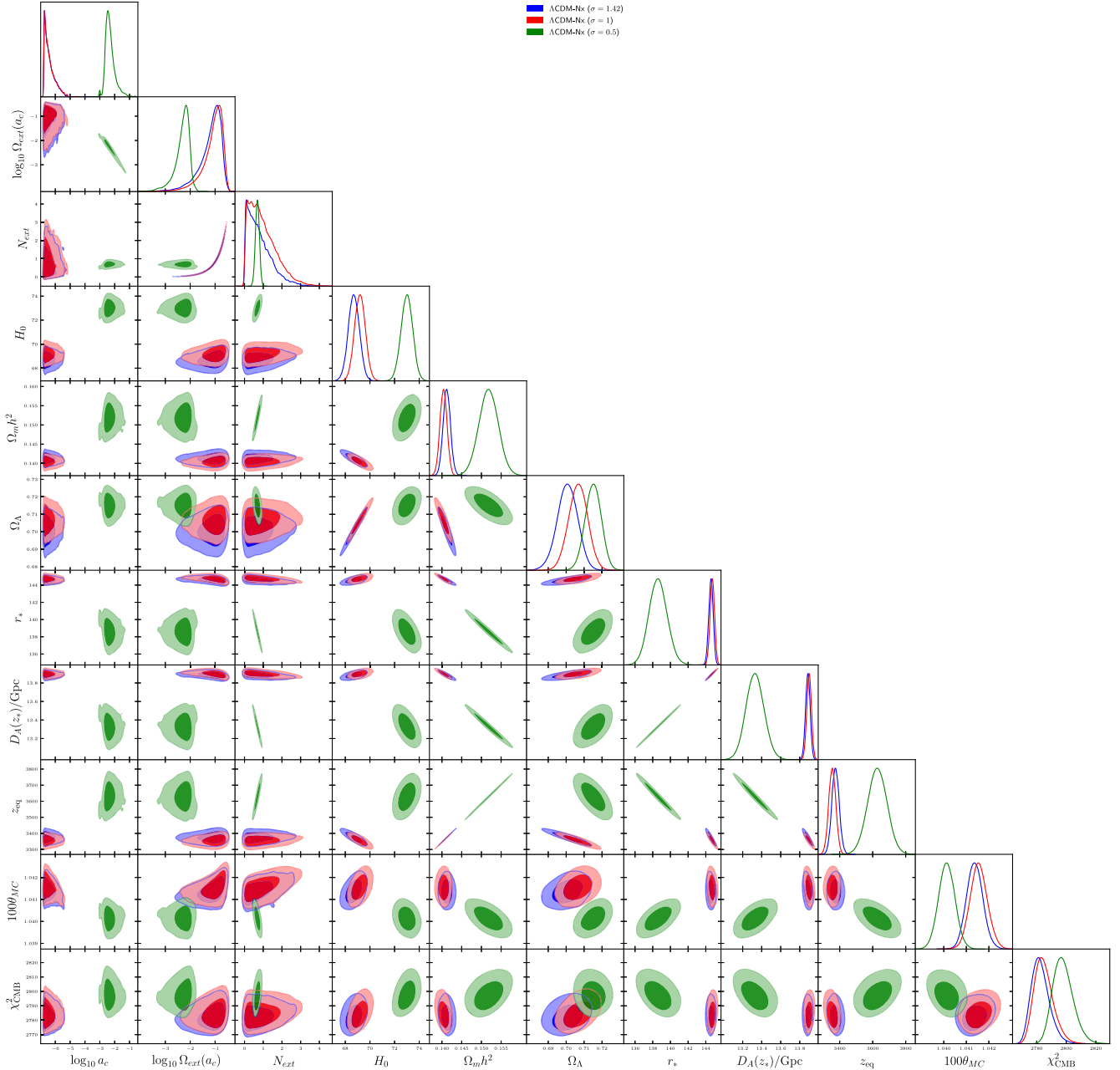


FIG. 3. Marginalized 68% and 95% parameter constraint contours for Λ CDM-Nx using *Planck* 2018 TT,TE,EE,lowE data and $H_0 = (74.03 \pm \sigma_H)$ km s $^{-1}$ Mpc $^{-1}$ with $\sigma_H = 1.42$ [R19] and the forecasting values $\sigma_H = 1, 0.5$.

in Fig. 3. We present in Fig. 4 the marginalized 68% and 95% parameter constraint contours for Λ CDM, with $\sigma_H = 1.42$, $\sigma_H = 0.5$ and No-Riess supplemented with Λ CDM-Nx with $\sigma_H = 0.5$. This last graph allows for a convenient comparison of the posteriors between Λ CDM models and Λ CDM-Nx with $\sigma_H = 0.5$ and the impact on the value of H_0 and other parameters.

The best-fit values for N_{ex} , $\Omega_{\text{ex}}(a_c)$, and the transition scale factor a_c for the three Λ CDM-Nx cases are $N_{\text{ex}} = 0.09$, $\Omega_{\text{ex}}(a_c) = 0.0035$, and $a_c = (7.1 \times 10^{-4})$ for H_0 with $\sigma_H = 1.42$, $N_{\text{ex}} = 0.07$, $\Omega_{\text{ex}}(a_c) = 0.0062$,

and $a_c = (1.5 \times 10^{-4})$ for H_0 with $\sigma_H = 1$, and $N_{\text{ex}} = 0.61$, $\Omega_{\text{ex}}(a_c) = 0.006$, and $a_c = (3.48 \times 10^{-3})$ for H_0 with $\sigma_H = 0.5$. Notice that $\Omega_{\text{ex}}(a_c)$ remains of the same order of magnitude in all three Λ CDM-Nx cases, while we get an increase of N_{ex} and a_c by factor of about 10 in Λ CDM-Nx with $\sigma_H = 0.5$ compared to Λ CDM-Nx with $\sigma_H = 1.42$ or $\sigma_H = 1$.

A. Analysis

Let us now compare and analyze the results of the MCMC analysis for the Λ CDM and Λ CDM-Nx models

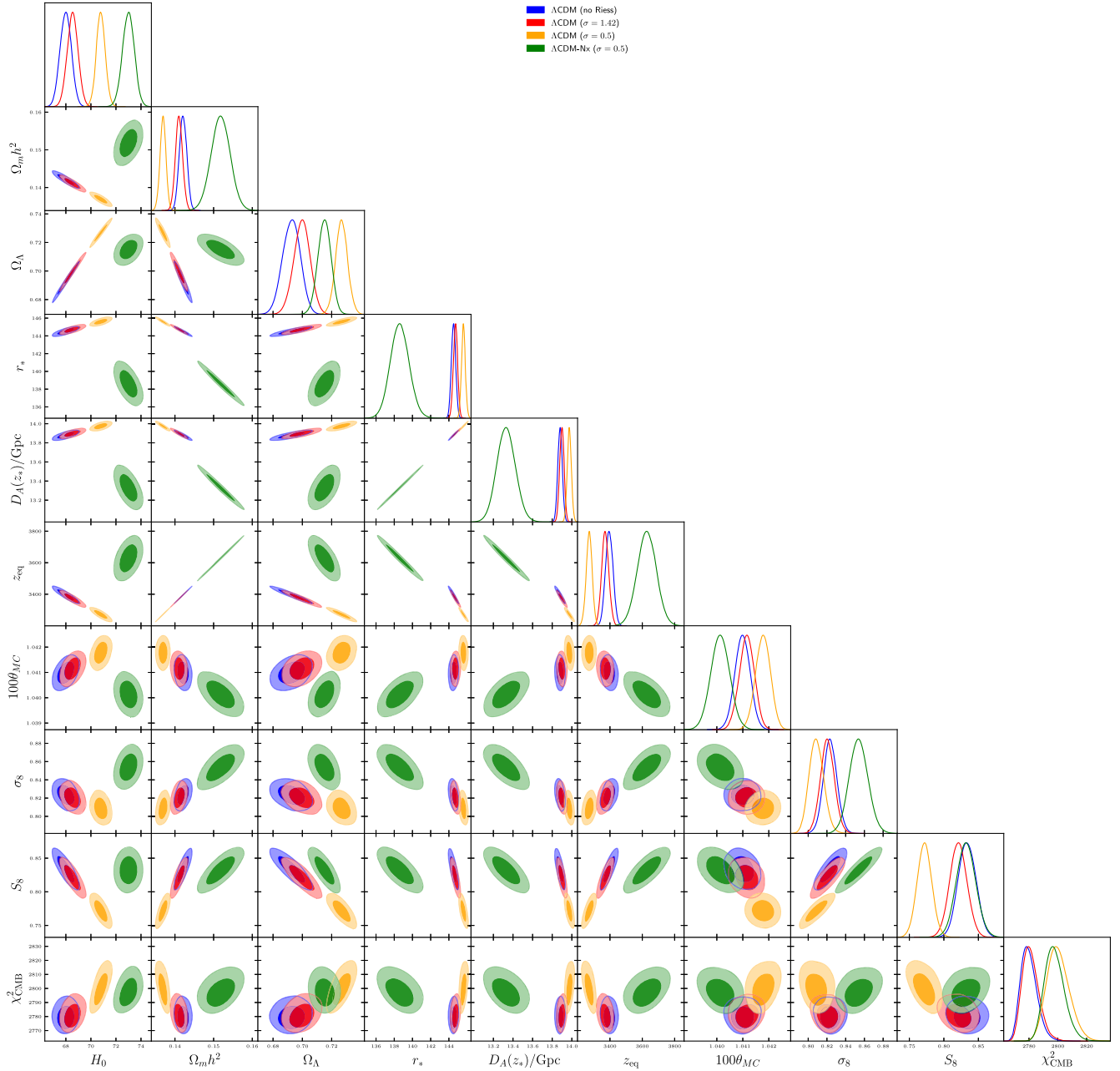


FIG. 4. Marginalized 68% and 95% parameter constraint contours using *Planck* 2018 TT,TE,EE,lowE data and $H_0 = (74.03 \pm 0.5) \text{ km s}^{-1} \text{ Mpc}^{-1}$ for $\Lambda\text{CDM-Nx}$ and $H_0 = (74.03 \pm \sigma_H) \text{ km s}^{-1} \text{ Mpc}^{-1}$ with $\sigma_H = 1.42$ [R19] and the forecasting values $\sigma_H = 0.5$ and No-Riess for ΛCDM models.

given in Tables I, II, and III. We present in Tables I, II, and III the best and sampling values for different cosmological parameters in the ΛCDM and $\Lambda\text{CDM-Nx}$ models and the corresponding figures of the constraint contours at 68% and 95% CL of different marginalized parameters, in Fig. 2 for ΛCDM , Fig. 3 for $\Lambda\text{CDM-Nx}$, and in Fig. 4 we incorporate ΛCDM and $\Lambda\text{CDM-Nx}$, we find it useful to analyze the difference between these cases by determining the relative difference and the percentage difference for some relevant parameters shown in Tables V and VI, respectively.

In Table IV we show the discrepancy between the value of $H_0 = 74.03 \pm \sigma_H$ for the three different values of σ_H (i.e., $\sigma_H = 1.42, 1, 0.5$), and the posterior probability of $H_0 \pm \sigma_s$, where σ_s is the 68% confidence level for ΛCDM and $\Lambda\text{CDM-Nx}$ from the MCMC analysis. The central value of H_0 of the samplings increases with decreasing σ_H , while the amplitude of σ_s remains nearly constant in all six cases ($\sigma_s \sim 0.42$). The quantity $\Delta H_0 \equiv (74.03 - H_0)$ corresponds to the distance between the central value $H_0 = 74.03$ from [R19] and the central value H_0 from each of the

TABLE IV. Central value H_0 and the 68% confidence level (σ_s) of the MCMC samplings using *Planck* 2018 and $H_0 = 74.02 \pm \sigma_H$ with different values of σ_H in the Λ CDM and Λ CDM-Nx models. The value $\sigma_H = 1.42$ corresponds to local measurements (R19), $\sigma_H = 1$ and $\sigma_H = 0.5$ are the two forecasting values of local H_0 measurements, and σ_s corresponds to the sampling margin at the 68% confidence level. We see that the central value of H_0 increases with decreasing σ_H , while the distance in $\Delta H_0/\sigma_T$ becomes smaller with $\sigma_T = \sigma_H + \sigma_s$. The reduction is far more prominent in Λ CDM-Nx than in Λ CDM. Finally, we show in the last two lines the χ^2 for H_0 and CMB sampling with the different data sets.

Model	Λ CDM	Λ CDM	Λ CDM	Λ CDM-Nx	Λ CDM-Nx	Λ CDM-Nx
$H_0 = 74.03 \pm \sigma_H$	$\sigma_H = 1.42$	$\sigma_H = 1$	$\sigma_H = 0.5$	$\sigma_H = 1.42$	$\sigma_H = 1$	$\sigma_H = 0.5$
$H_0 \pm \sigma_s$	68.54 ± 0.43	69.04 ± 0.41	70.79 ± 0.36	68.70 ± 0.45	69.19 ± 0.44	72.99 ± 0.47
$\sigma_T = \sigma_H + \sigma_s$	$1.42 + 0.43$	$1 + 0.41$	$0.5 + 0.36$	$1.42 + 0.45$	$1 + 0.44$	$0.5 + 0.36$
$\Delta H_0/\sigma_T$	2.968	2.697	1.820	2.850	2.602	0.550
$\chi^2_{H_0}$	15.0 ± 2.4	25 ± 4	42 ± 9	14.2 ± 2.4	24 ± 4	5.2 ± 4.2

TABLE V. In the second line we show the best-fit values for Λ CDM-Nx with $H_0 = (1.42 \pm 0.5) \text{ km s}^{-1} \text{ Mpc}^{-1}$ and we present the relative percent difference $\Delta_{\text{RPD}}P \equiv 100(P_\Lambda - P_{N_x})/P_{N_x}$ for different parameters between the Λ CDM-Nx (with $\sigma_H = 0.5$) and Λ CDM models for different values of $\sigma_H = 0.5, 1.42$, and No-Riess.

Model	$100\theta(z_*)$	$D_A(r_*)$	r_*	H_0	$\Omega_m h^2$	z_{eq}	σ_8	S_8	$\chi^2_{H_0}$	χ^2_{CMB}	$(\chi_{\text{CMB}}^{\text{red}})^2$
Λ CDM-Nx $\sigma_H = 0.5$	1.04027	13.404	139.40	72.83	0.1499	3581.23	0.847	0.822	5.72	2779.81	1.100
Λ CDM $\sigma_H = 0.5$	0.146	4.239	4.429	-2.809	-8.612	-8.615	-4.591	-6.156	635.111	0.167	0.088
Λ CDM $\sigma_H = 1.42$	0.082	3.688	3.815	-5.873	-5.892	-5.894	-3.062	-0.094	159.815	-0.508	-0.587
Λ CDM No-Riess	0.068	3.525	3.639	-6.691	-5.115	-5.117	-2.748	1.524	...	-0.556	-0.635

samplings, and we define $\sigma_T \equiv \sigma_H + \sigma_s$ for each case. Not surprisingly, for smaller values of σ_H we obtain a larger H_0 and a decrease in $\Delta H_0/\sigma_T$ in the Λ CDM and Λ CDM-Nx models. However, even though the value of H_0 increases, so does $\chi^2_{H_0}$ in all cases except for Λ CDM-Nx with $\sigma_H = 0.5$. We obtain in the Λ CDM model $\chi^2_{H_0} = 15 \pm 2.4$ for $\sigma_H = 1.42$, $\chi^2_{H_0} = 25 \pm 4$ for $\sigma_H = 1$, and $\chi^2_{H_0} = 42 \pm 9$ for $\sigma_H = 0.5$, in Λ CDM-Nx we have $\chi^2_{H_0} = 14.2 \pm 2.4$ for $\sigma_H = 1.42$ and $\chi^2_{H_0} = 24 \pm 4$ for $\sigma_H = 1$, while we have a significant reduction in the $\sigma_H = 0.5$ model, obtaining $\chi^2_{H_0} = 5.2 \pm 4.2$. Notice that the difference in $\chi^2_{H_0}$ between Λ CDM and Λ CDM-Nx is small for $\sigma_H = 1.42$ and $\sigma_H = 1$; however, the impact from the Λ CDM-Nx model with the forecasting value $\sigma_H = 0.5$ has a significant reduction in $\chi^2_{H_0}$ from $\chi^2_{H_0} = 42 \pm 9$ in Λ CDM to $\chi^2_{H_0} = 5.2 \pm 4.2$ in Λ CDM-Nx. We remark that only Λ CDM-Nx with $\sigma_H = 0.5$ has a $\Delta H_0/\sigma_T$ smaller than one, clearly showing the impact of the reduced σ_H .

In order to assess the impact of the reduced forecasting value $\sigma_H = 0.5$ in Λ CDM-Nx on different cosmological parameters, we compare the results from Λ CDM-Nx with $\sigma_H = 0.5$ and Λ CDM with $\sigma_H = 1.42, \sigma_H = 0.5$, and No-Riess in Table V and we determine the relative percent difference between Λ CDM-Nx with $\sigma_H = 0.5$ with Λ CDM for several parameters, and we show in Table VI the percentage difference of several parameters between Λ CDM-Nx with $\sigma_H = 0.5$

and Λ CDM-Nx with $\sigma_H = 1$ and $\sigma_H = 1.42$ as well as Λ CDM with $\sigma_H = 0.5, \sigma_H = 0.5 = 1, \sigma_H = 1.42$, and No-Riess.

In Table V we present the relative percent difference (RPD) $\Delta_{\text{RPD}}P \equiv 100(P_\Lambda - P_{N_x})/P_{N_x}$ for several parameters between the Λ CDM-Nx (with $\sigma_H = 0.5$) and Λ CDM models (with $\sigma_H = 0.5, \sigma_H = 1.42$, and No-Riess). Not surprisingly, the change in θ is small (with $\Delta_{\text{RPD}}\theta < 0.15\%$), we get a decrease in $D_A(r_*)$ and $r(r_*)$ of the same order with $\Delta_{\text{RPD}} \sim 4\%$ for both quantities, while we have $\Delta_{\text{RPD}}H_0$ values of 6.7%, 5.9%, and 2.8% with respect to Λ CDM (No-Riess, $\sigma_H = 1.42$, and $\sigma_H = 0.5$, respectively). In the last column we present the reduced $(\chi_{\text{CMB}}^{\text{red}})^2$, with $(\chi_{\text{CMB}}^{\text{red}})^2 = \chi^2_{\text{CMB}}/(N_{\text{d.o.f.}} - N_{\text{param}})$, and we take into account that Λ CDM-Nx has two extra parameters, namely, a_c and $\Omega_{\text{ex}}(a_c)$. We obtain a slight increase in $(\chi_{\text{CMB}}^{\text{red}})^2$ of less than 1% for Λ CDM-Nx with $\sigma_H = 0.5$ vs Λ CDM (0.635% against Λ CDM No-Riess and 0.587% in Λ CDM with $\sigma_H = 1.42$ models). On the other hand, we obtain a significant reduction in $\chi^2_{H_0}$ for Λ CDM-Nx ($\sigma_H = 0.5$), corresponding to a $\Delta_{\text{RPD}}\chi^2_{H_0}$ of 635% vs Λ CDM ($\sigma_H = 0.5$) and 159% vs Λ CDM ($\sigma_H = 1.42$).

In Table VI we show in the first two lines the value of H_0 and the distance between obtained best-fit values of H_0 and the central value of $H_0 = 74.03$ [R19] divided by the observational error $\sigma_H = 1.42$ for each of the different cases, while in the third line we present the

TABLE VI. We show in the top part the values of H_0 , its distance to H_R in units of $\sigma_R = 1.42$, and the reduced χ^2_{CMB} for the different $\Lambda\text{CDM-N}_x$ and ΛCDM cases. In the bottom part we present the percentage difference (% Diff.) defined as $\Delta P \equiv 100 (P - P_{N_x}(\sigma_H = 0.5)) / [(P + P_{N_x}(\sigma_H = 0.5)) / 2]$ of the parameters between $\Lambda\text{CDM-N}_x$ (with $\sigma_H = 0.5$) and the different $\Lambda\text{CDM-N}_x$ and ΛCDM cases.

Best-fit models	$\Lambda\text{CDM-N}_x$	$\Lambda\text{CDM-N}_x$	$\Lambda\text{CDM-N}_x$	ΛCDM	ΛCDM	ΛCDM	ΛCDM
$H_0 = 74.03 \pm \sigma_H$	$\sigma_H = 0.5$	$\sigma_H = 1.42$	$\sigma_H = 1$	No-Riess	$\sigma_H = 1.42$	$\sigma_H = 1$	$\sigma_H = 0.5$
H_0	72.83	69.14	69.23	67.96	68.56	69.05	70.79
$(H_R - H_0)/1.42$	0.83	3.43	3.37	4.27	3.85	3.50	2.28
$(\chi^2_{\text{CMB}})^{\text{red}}$	1.100	1.095	1.095	1.093	1.094	1.094	1.101
Parameter	$\Lambda\text{CDM-N}_x$	% Diff.	% Diff.	% Diff.	% Diff.	% Diff.	% Diff.
H_0	72.83	-1.30	-1.27	-1.73	-1.51	-1.33	0.71
Ω_Λ	-0.72	-0.53	-0.43	-0.90	-0.62	-0.40	-0.32
Ω_m	0.28	1.29	1.07	2.15	1.51	1.00	0.83
$\Omega_m h^2$	0.15	-1.31	-1.47	-1.31	1.51	-1.67	-2.25
$\Omega_b h^2$	0.02	-0.55	-0.33	-0.66	-0.54	-0.41	-0.07
z_{eq}	3581.23	-1.31	-1.47	-1.31	-1.52	-1.67	-2.25
σ_8	0.85	-0.63	-0.64	-0.70	-0.78	-0.87	-1.17
S_8	0.82	0.01	-0.10	0.38	-0.02	-0.37	-1.59
z_{drag}	1062.30	0.64	-0.04	-0.06	-0.05	-0.05	-0.04
r_{drag}	141.80	0.83	0.89	0.92	0.96	0.98	1.08
z_*	1090.31	-0.70	-0.02	-0.01	-0.02	-0.02	-0.04
r_*	139.40	0.81	0.87	0.89	0.94	0.96	1.08
$D_A(r_*)$	13.40	0.78	0.84	0.87	0.91	0.93	1.04
$100\theta(z_*)$	1.04027	0.02	0.03	0.02	0.02	0.02	0.04
$\chi^2_{H_0}$	5.72	17.44	30.11	...	22.21	31.26	38.03
χ^2_{CMB}	2779.81	-0.122	-0.115	-0.139	-0.127	-0.121	0.042
$(\chi^2_{\text{CMB}})^{\text{red}}$	1.100	-0.122	-0.115	-0.159	-0.147	-0.140	0.022

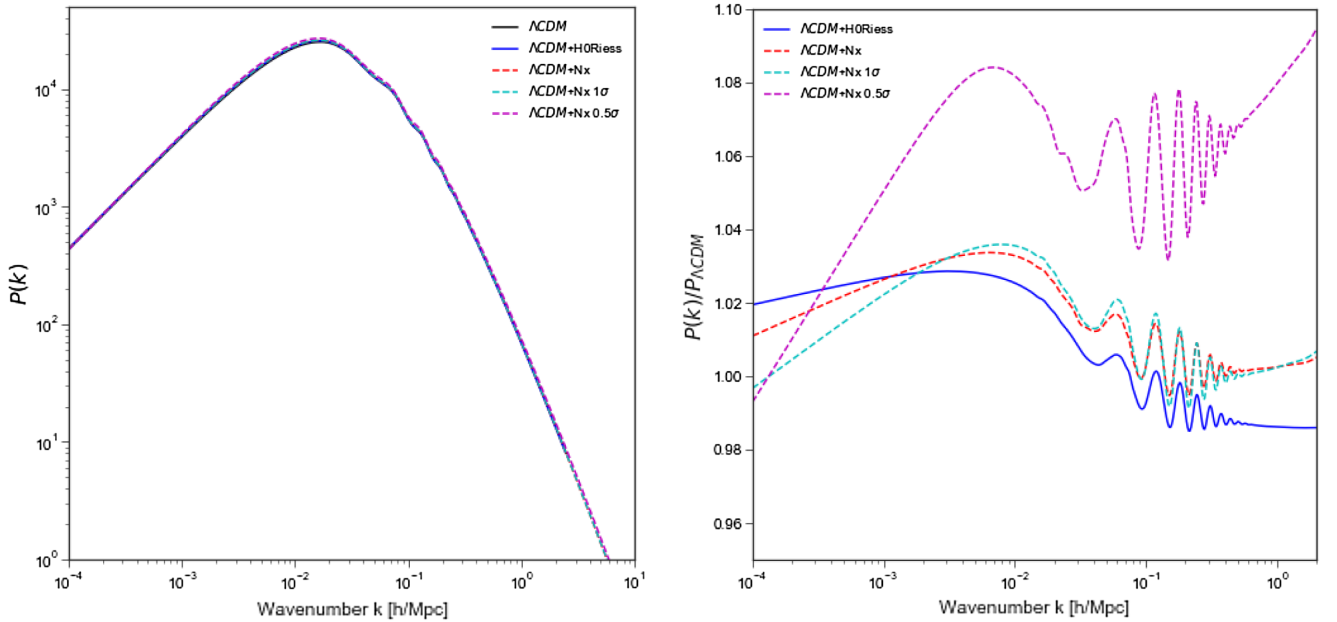


FIG. 5. Matter power spectrum (left panel) for ΛCDM and $\Lambda\text{CDM-N}_x$ and the ratios (right panel) $\Lambda\text{CDM-N}_x/\Lambda\text{CDM}$ and $\Lambda\text{CDM-No-Riess}/\Lambda\text{CDM}$, where $1\sigma \equiv 1 \text{ km s}^{-1} \text{ Mpc}^{-1}$ and $0.5\sigma \equiv 0.5 \text{ km s}^{-1} \text{ Mpc}^{-1}$.

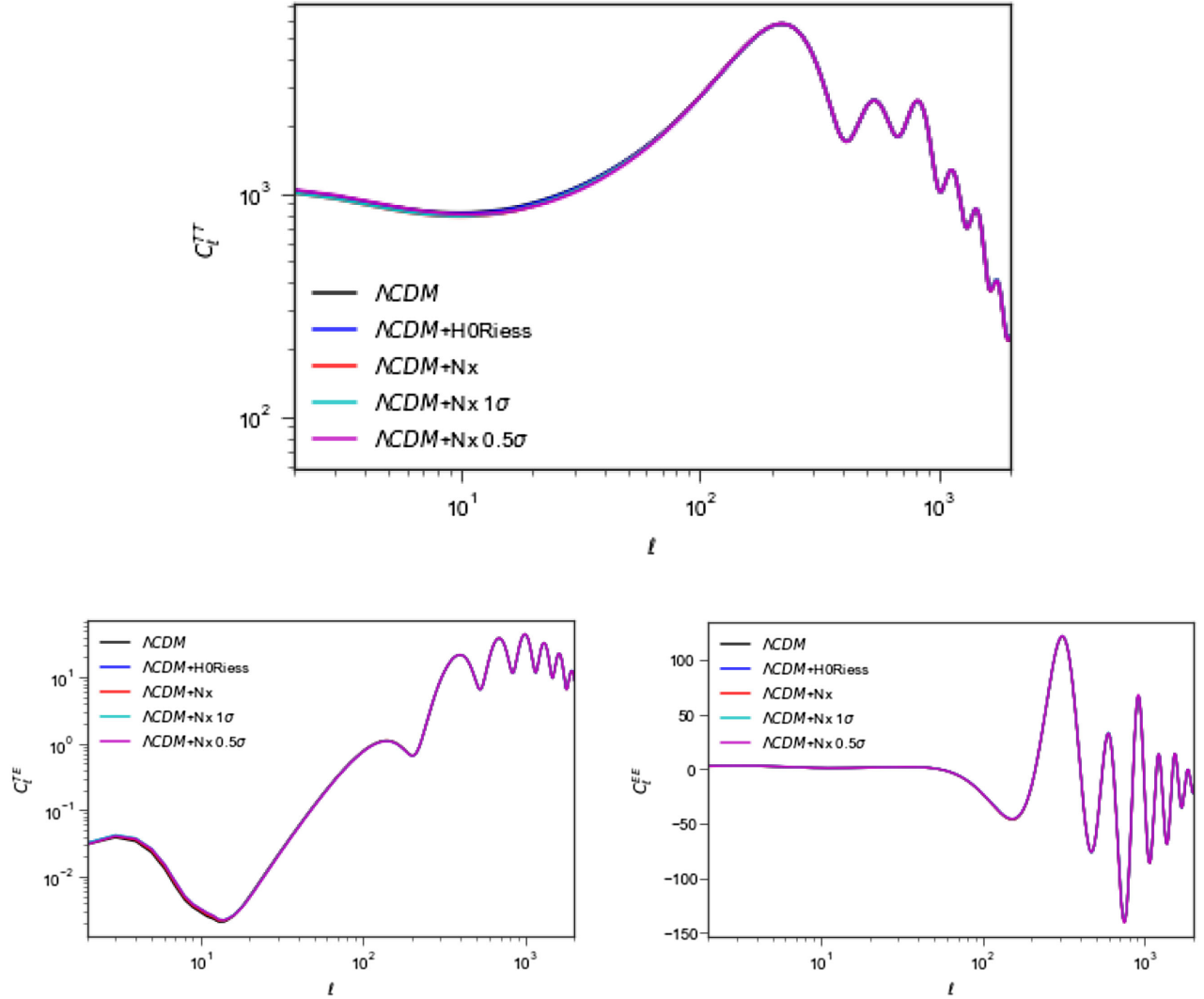


FIG. 6. We plot CMB_l^{TT} , CMB_l^{TE} , CMB_l^{EE} power spectra for ΛCDM and $\Lambda\text{CDM-Nx}$ models, where $1\sigma \equiv 1 \text{ km s}^{-1} \text{ Mpc}^{-1}$ and $0.5\sigma \equiv 0.5 \text{ km s}^{-1} \text{ Mpc}^{-1}$.

reduced $(\chi_{\text{CMB}}^{\text{red}})^2$. We also show the percentage difference $\Delta P \equiv 100 [(P - P_{N_{x0.5}})/(P + P_{N_{x0.5}})]/2$ for different cosmological parameters, between $\Lambda\text{CDM-Nx}$ ($\sigma_H = 0.5$) and the other six cases considered in this work, i.e., $\Lambda\text{CDM-Nx}$ ($\sigma_H = 1.42$ and $\sigma_H = 1$) and ΛCDM ($\sigma_H = 1.42$, $\sigma_H = 1$, $\sigma_H = 0.5$, and No-Riess). Notice that the changes in r_* and $D_A(\star)$ are of the same magnitude (around $\sim 0.90\%$), while the percentage change in $100\theta(z_*)$ is small (around $\sim 0.02\%$). We find a significant increase in the $\chi_{H_0}^2$ values of the six cases compared to $\Lambda\text{CDM-Nx}$ ($\sigma_H = 0.5$), with a percentage of $\Delta P(\chi_{H_0}^2) = 22.21$ against ΛCDM ($\sigma_H = 1.42$) and $\Delta P(\chi_{H_0}^2) = 38.03$ against $\Lambda\text{CDM-Nx}$ ($\sigma_H = 0.5$), while we obtain a reduction in the CMB χ^2 of $\Delta P[(\chi_{\text{CMB}}^{\text{red}})^2] = 0.127(0.121)$ with respect to ΛCDM $\sigma_H = 1.42$ ($\Lambda\text{CDM}\sigma_H = 1$) and an increase of $\Delta P[(\chi_{\text{CMB}}^{\text{red}})^2] = -0.042$ compared to ΛCDM ($\sigma_H = 0.5$).

B. Matter power spectrum and CMB power spectrum

Here we show the impact of a rapid diluted energy density on the matter power spectrum of a rapid diluted energy density given by $\Omega_{\text{ex}}(a_c)$ at a_c with and at a mode $k_c \equiv a_c H_c$ with $H_c \equiv H(a_c)$. As shown in Sec. III C, a rapid diluted energy density generates a bump in the ratio of the matter power spectrum between the $\Lambda\text{CDM-Nx}$ and ΛCDM models [66], as observed in Refs. [25,33,43,44,57,58,62,63,65,73,74]. In Fig. 5 we show the matter power spectrum. On the left-hand side we plot ΛCDM with and without Riess data [R19] and the three $\Lambda\text{CDM-Nx}$ cases ($\sigma_H = 1.42$, $\sigma_H = 1$, $\sigma_H = 0.5$). On the right-hand side we show the ratios of $\Lambda\text{CDM-Nx}/\Lambda\text{CDM}$ and $\Lambda\text{CDM-No-Riess}/\Lambda\text{CDM}$. Notice that for $\Lambda\text{CDM-Nx}$ with $\sigma_H = 0.5$ we find an increase in power of about 6% for modes $10^{-3} < k < 1$ in h/Mpc units, while for the other ΛCDM models ($\sigma_H = 1.42$ and $\sigma_H = 1$) the difference is below 2%. In Fig. 6 we show the CMB power

spectrum for all five models described above, top panel corresponds to C_l^{TT} , left bottom panel C_l^{TE} and C_L^{EE} right bottom panel.

V. CONCLUSIONS

We have studied possible solutions to the increasing H_0 tension between local H_0 and *Planck* CMB measurements in the context of the Λ CDM model. Recent local measurements of H_0 estimate a value of $H_0 = 74.03 \pm 1.42 \text{ km s}^{-1} \text{ Mpc}^{-1}$ [4], with a reported average value for different local measurements of $H_0 = (73.03 \pm 0.8) \text{ km s}^{-1} \text{ Mpc}^{-1}$ [14], while *Planck* obtained a value of $H_0 = (67.36 \pm 0.54) \text{ km s}^{-1} \text{ Mpc}^{-1}$ [9]. The magnitude of the tension between the early- and late-time measurements either implies an important misunderstanding in the systematic errors of the observational analysis, or it may hint towards new physics beyond the concordance cosmological Λ CDM model. Here we took the second point of view and studied possible solutions to reduce the tension between local H_0 measurements and the CMB radiation observed by the *Planck* satellite. To alleviate this discrepancy, we added to Λ CDM an extra-relativistic energy density ρ_{ex} present at early times, and we allowed for ρ_{ex} to dilute rapidly (as $\rho_{\text{ex}} \propto 1/a^6$) for a scale factor larger than a_c ; we named this model Λ CDM-Nx. These types of dynamics are present in some scalar field models (quintessence fields) and have been widely studied. With these two phenomenological parameters, we analyzed Λ CDM-Nx using CMB data [P18] and local H_0 measurements [R19]. Besides taking $H_0 = (74.03 \pm \sigma_H) \text{ km s}^{-1} \text{ Mpc}^{-1}$ with $\sigma_H = 1.42$ [R19], we also included two forecasting 1σ standard deviation values, $\sigma_H = 1$ and $\sigma_H = 0.5 \text{ km s}^{-1} \text{ Mpc}^{-1}$, and we assessed the impact of these forecasting H_0 measurements on the posterior probabilities of the different cosmological parameters.

For Λ CDM-Nx, using *Planck* 2018 CMB (TT, TE, EE + lowE) data and the forecasting local measurement $H_0 = 74.03 \pm 0.5 \text{ km s}^{-1} \text{ Mpc}^{-1}$, we obtained a value for the Hubble parameter of $H_0 = 72.99 \pm 0.47 \text{ km s}^{-1} \text{ Mpc}^{-1}$ at 68% C.L. with a best-fit $H_0 = 72.83 \text{ km s}^{-1} \text{ Mpc}^{-1}$. In Table VI we show the percentage difference of several cosmological parameters in the Λ CDM-Nx model with a forecasting value $H_0 = (74.03 \pm 0.5) \text{ km s}^{-1} \text{ Mpc}^{-1}$ and the other six models considered in this work.

In particular, we found it interesting to compare Λ CDM-Nx with $\sigma_H = 0.5$ with Λ CDM $\sigma_H = 0.5$ and Λ CDM $\sigma_H = 1.42$ models. We found an increase in the percentage difference between the two Λ CDM models of 22.21% for $\sigma_H = 1.42$ and 38.03% for $\sigma_H = 0.5$ in $\chi_{H_0}^2$, respectively, while we obtained a decrease in the reduced $\chi_{\text{CMB}}^{\text{red}}$ of 0.147% for Λ CDM $\sigma_H = 1.42$ and a negligible increase of 0.022% in the Λ CDM $\sigma_H = 0.5$ model.

Not surprisingly, a reduced 1σ ($\sigma_H = 0.5$) in the forecasting value of H_0 has a larger impact on the posterior value of H_0 than in the analysis of the CMB. Notice, however, that the change in $\chi_{\text{CMB}}^{\text{red}}$ is 2 orders of magnitude smaller than the change in $\chi_{H_0}^2$.

To conclude, we found that a Λ CDM-Nx model, with extra-relativistic energy density at a scale factor $a < a_c$, is consistent with H_0 [R19] and CMB [P18] observations as long as we assume a small forecasting value or H_0 data (e.g., $\sigma_H = 0.5 \text{ km s}^{-1} \text{ Mpc}^{-1}$), while the impact on the CMB χ^2 is small. Finally, we would like to stress that our phenomenological model Λ CDM-Nx, and in particular the ρ_{ex} and a_c parameters, may have a sound derivation from extension of the standard model of particle physics as for example in BDE or EDE models. These are exciting times to pursue a deeper understanding of our Universe, in an epoch of high-precision cosmological observations thanks to DESI and in the near future LSST, to further constrain the building blocks of particle physics through their impact on cosmological observables.

ACKNOWLEDGMENTS

Axel de la Macorra acknowledges support from Project IN105021, Programa de Apoyo a Proyectos de Investigación e Innovación Tecnológica (PAPIIT) Universidad Nacional Autónoma de México (UNAM), and a sabbatical grant from Programa de Apoyos para la Superación del Personal Académico (PASPA) of the Dirección General del Personal Académico (DGAPA) of Universidad Nacional Autónoma de México (UNAM) and Consejo Nacional de Ciencia y Tecnología (Conacyt). Johanna Garrido acknowledges postgraduate scholarship from Conacyt. Erick Almaraz acknowledges the support of a Postdoctoral scholarship by Conacyt. We also thank Mariana Jaber and Jorge Mastache for useful discussions.

[1] Boudewijn F. Roukema and Yuzuru Yoshii, The failure of simple merging models to save a flat, $\Omega_0 = 1$ universe, *Astrophys. J.* **418**, L1 (1993).

[2] Adam G. Riess *et al.*, Observational evidence from supernovae for an accelerating universe and a cosmological constant, *Astron. J.* **116**, 1009 (1998).

- [3] S. Perlmutter *et al.*, Measurements of α and Λ from 42 high redshift supernovae, *Astrophys. J.* **517**, 565 (1999).
- [4] Adam G. Riess, Stefano Casertano, Wenlong Yuan, Lucas M. Macri, and Dan Scolnic, Large magellanic cloud cepheid standards provide a 1% foundation for the determination of the Hubble constant and stronger evidence for physics beyond Λ CDM, *Astrophys. J.* **876**, 85 (2019).
- [5] A. G. Riess, L. M. Macri, S. L. Hoffmann, D. Scolnic, S. Casertano, A. V. Filippenko, B. E. Tucker, M. J. Reid, D. O. Jones, J. M. Silverman, R. Chornock, P. Challis, W. Yuan, P. J. Brown, and R. J. Foley, A 2.4% determination of the local value of the hubble constant, *Astrophys. J.* **826**, 56 (2016).
- [6] Adam G. Riess *et al.*, Milky way cepheid standards for measuring cosmic distances and application to Gaia DR2: Implications for the Hubble constant, *Astrophys. J.* **861**, 126 (2018).
- [7] Rachael L. Beaton *et al.*, The Carnegie-Chicago Hubble program. I. An independent approach to the extragalactic distance scale using only population II distance indicators, *Astrophys. J.* **832**, 210 (2016).
- [8] Wendy L. Freedman *et al.*, The Carnegie-Chicago Hubble program. VIII. An independent determination of the Hubble constant based on the tip of the red giant branch, *Astrophys. J.* **882**, 34 (2019).
- [9] N. Aghanim *et al.*, Planck 2018 results. VI. Cosmological parameters, *Astron. Astrophys.* **641**, A6 (2020).
- [10] V. Bonvin *et al.*, H0LiCOW—V. New COSMOGRAIL time delays of HE 0435 – 1223: H_0 to 3.8 per cent precision from strong lensing in a flat Λ CDM model, *Mon. Not. R. Astron. Soc.* **465**, 4914 (2017).
- [11] S. Birrer *et al.*, H0LiCOW—IX. Cosmographic analysis of the doubly imaged quasar SDSS 1206 + 4332 and a new measurement of the Hubble constant, *Mon. Not. R. Astron. Soc.* **484**, 4726 (2019).
- [12] Kenneth C. Wong *et al.*, H0LiCOW XIII. A 2.4% measurement of H_0 from lensed quasars: 5.3σ tension between early and late-Universe probes, *Mon. Not. R. Astron. Soc.* **498**, 1420 (2020).
- [13] P. A. Zyla *et al.*, Review of particle physics, *Prog. Theor. Exp. Phys.* **2020**, 083C01 (2020).
- [14] L. Verde, T. Treu, and A. G. Riess, Tensions between the early and the late universe, *Nat. Astron.* **3**, 891 (2019).
- [15] D. W. Pesce *et al.*, The Megamaser cosmology project. XIII. Combined Hubble constant constraints, *Astrophys. J. Lett.* **891**, L1 (2020).
- [16] S. Birrer, A. J. Shajib, A. Galan, M. Millon, T. Treu, A. Agnello, M. Auger, G. C. F. Chen, L. Christensen, T. Collett *et al.*, TDCOSMO—IV. Hierarchical time-delay cosmography—Joint inference of the Hubble constant and galaxy density profiles, *Astron. Astrophys.* **643**, A165 (2020).
- [17] Simone Aiola *et al.*, The Atacama Cosmology Telescope: DR4 maps and cosmological parameters, *J. Cosmol. Astropart. Phys.* **12** (2020) 047.
- [18] G. E. Addison, Y. Huang, D. J. Watts, C. L. Bennett, M. Halpern, G. Hinshaw, and J. L. Weiland, Quantifying discordance in the 2015 Planck CMB spectrum, *Astrophys. J.* **818**, 132 (2016).
- [19] Kevin Aylor, MacKenzie Joy, Lloyd Knox, Marius Millea, Srinivasan Raghunathan, and W. L. Kimmy Wu, Sounds discordant: Classical distance ladder & Λ CDM -based determinations of the cosmological sound horizon, *Astrophys. J.* **874**, 4 (2019).
- [20] George Efstathiou, H_0 revisited, *Mon. Not. R. Astron. Soc.* **440**, 1138 (2014).
- [21] Lloyd Knox and Marius Millea, The Hubble hunter’s guide, *Phys. Rev. D* **101**, 043533 (2020).
- [22] Vivian Poulin, Tristan L. Smith, Tanvi Karwal, and Marc Kamionkowski, Early Dark Energy Can Resolve The Hubble Tension, *Phys. Rev. Lett.* **122**, 221301 (2019).
- [23] Tanvi Karwal and Marc Kamionkowski, Dark energy at early times, the Hubble parameter, and the string axiverse, *Phys. Rev. D* **94**, 103523 (2016).
- [24] Jeremy Sakstein and Mark Trodden, Early Dark Energy from Massive Neutrinos—A Natural Resolution of the Hubble Tension, *Phys. Rev. Lett.* **124**, 161301 (2020).
- [25] Lloyd Knox and Marius Millea, Hubble constant hunter’s guide, *Phys. Rev. D* **101**, 043533 (2020).
- [26] Eleonora Di Valentino, Alessandro Melchiorri, Olga Mena, and Sunny Vagnozzi, Interacting dark energy in the early 2020s: A promising solution to the H_0 and cosmic shear tensions, *Phys. Dark Universe* **30**, 100666 (2020).
- [27] Katherine Freese and Martin Wolfgang Winkler, Chain early dark energy: Solving the Hubble tension and explaining today’s dark energy, *Phys. Rev. D* **104**, 083533 (2021).
- [28] Riccardo Murgia, Guillermo F. Abellán, and Vivian Poulin, Early dark energy resolution to the Hubble tension in light of weak lensing surveys and lensing anomalies, *Phys. Rev. D* **103**, 063502 (2021).
- [29] Florian Niedermann and Martin S. Sloth, Resolving the Hubble tension with new early dark energy, *Phys. Rev. D* **102**, 063527 (2020).
- [30] Eleonora Di Valentino, Olga Mena, Supriya Pan, Luca Visinelli, Weiqiang Yang, Alessandro Melchiorri, David F. Mota, Adam G. Riess, and Joseph Silk, In the realm of the Hubble tension – A review of solutions, *Classical Quantum Gravity* **38**, 153001 (2021).
- [31] Eleonora Di Valentino *et al.*, Snowmass2021—Letter of interest cosmology intertwined II: The Hubble constant tension, *Astropart. Phys.* **131**, 102605 (2021).
- [32] J. Colin Hill, Evan McDonough, Michael W. Toomey, and Stephon Alexander, Early dark energy does not restore cosmological concordance, *Phys. Rev. D* **102**, 043507 (2020).
- [33] Anatoly Klypin, Vivian Poulin, Francisco Prada, Joel Primack, Marc Kamionkowski, Vladimir Avila-Reese, Aldo Rodríguez-Puebla, Peter Behroozi, Doug Hellinger, and Tristan L. Smith, Clustering and halo abundances in early dark energy cosmological models, *Mon. Not. R. Astron. Soc.* **504**, 769 (2021).
- [34] Mikhail M. Ivanov, Evan McDonough, J. Colin Hill, Marko Simonović, Michael W. Toomey, Stephon Alexander, and Matias Zaldarriaga, Constraining early dark energy with large-scale structure, *Phys. Rev. D* **102**, 103502 (2020).
- [35] Jose Luis Bernal, Licia Verde, and Adam G. Riess, The trouble with H_0 , *J. Cosmol. Astropart. Phys.* **10** (2016) 019.
- [36] Eleonora Di Valentino, Alessandro Melchiorri, Olga Mena, and Sunny Vagnozzi, Nonminimal dark sector physics and cosmological tensions, *Phys. Rev. D* **101**, 063502 (2020).
- [37] Supriya Pan, Weiqiang Yang, Eleonora Di Valentino, Emmanuel N. Saridakis, and Subenoy Chakraborty,

- Interacting scenarios with dynamical dark energy: Observational constraints and alleviation of the H_0 tension, *Phys. Rev. D* **100**, 103520 (2019).
- [38] Eleonora Di Valentino, Ankan Mukherjee, and Anjan A. Sen, Dark energy with phantom crossing and the H_0 tension, *Entropy* **23**, 404 (2021).
- [39] Adriá Gómez-Valent, Valeria Pettorino, and Luca Amendola, Update on coupled dark energy and the H_0 tension, *Phys. Rev. D* **101**, 123513 (2020).
- [40] Guillermo Ballesteros, Alessio Notari, and Fabrizio Rompineve, The H_0 tension: ΔG_N vs. ΔN_{eff} , 4 2020.
- [41] Christina D. Kreisch, Francis-Yan Cyr-Racine, and Olivier Dor, The neutrino puzzle: Anomalies, interactions, and cosmological tensions, *Phys. Rev. D* **101**, 123505 (2020).
- [42] Eric V. Linder and Georg Robbers, Shifting the universe: Early dark energy and standard rulers, *J. Cosmol. Astropart. Phys.* **06** (2008) 004.
- [43] Matthew J. Francis, Geraint F. Lewis, and Eric V. Linder, Can early dark energy be detected in non-linear structure?, *Mon. Not. R. Astron. Soc.* **394**, 605 (2009).
- [44] Erminia Calabrese, Roland de Putter, Dragan Huterer, Eric V. Linder, and Alessandro Melchiorri, Future CMB constraints on early, cold, or stressed dark energy, *Phys. Rev. D* **83**, 023011 (2011).
- [45] Stephen A. Appleby, Eric V. Linder, and Jochen Weller, Cluster probes of dark energy clustering, *Phys. Rev. D* **88**, 043526 (2013).
- [46] Adam G. Riess *et al.*, New Hubble space telescope discoveries of Type Ia supernovae at $z \geq 1$: Narrowing constraints on the early behavior of dark energy, *Astrophys. J.* **659**, 98 (2007).
- [47] Michael Doran and Georg Robbers, Early dark energy cosmologies, *J. Cosmol. Astropart. Phys.* **06** (2006) 026.
- [48] Rachel Bean, Steen H. Hansen, and Alessandro Melchiorri, Early universe constraints on a primordial scaling field, *Phys. Rev. D* **64**, 103508 (2001).
- [49] Paul J. Steinhardt, Li-Min Wang, and Ivaylo Zlatev, Cosmological tracking solutions, *Phys. Rev. D* **59**, 123504 (1999).
- [50] Ivaylo Zlatev, Li-Min Wang, and Paul J. Steinhardt, Quintessence, Cosmic Coincidence, and the Cosmological Constant, *Phys. Rev. Lett.* **82**, 896 (1999).
- [51] A. de la Macorra and G. Piccinelli, General scalar fields as quintessence, *Phys. Rev. D* **61**, 123503 (2000).
- [52] Axel de la Macorra, A realistic particle physics dark energy model, *Phys. Rev. D* **72**, 043508 (2005).
- [53] A. de la Macorra and C. Stephan-Otto, Natural Quintessence with Gauge Coupling Unification, *Phys. Rev. Lett.* **87**, 271301 (2001).
- [54] A. de la Macorra and C. Stephan-Otto, Quintessence restrictions on negative power and condensate potentials, *Phys. Rev. D* **65**, 083520 (2002).
- [55] R. R. Caldwell and Eric V. Linder, The Limits of Quintessence, *Phys. Rev. Lett.* **95**, 141301 (2005).
- [56] Eric V. Linder, The dynamics of quintessence, the quintessence of dynamics, *Gen. Relativ. Gravit.* **40**, 329 (2008).
- [57] Erminia Calabrese, Dragan Huterer, Eric V. Linder, Alessandro Melchiorri, and Luca Pagano, Limits on dark radiation, early dark energy, and relativistic degrees of freedom, *Phys. Rev. D* **83**, 123504 (2011).
- [58] Johan Samsing, Eric V. Linder, and Tristan L. Smith, Model independent early expansion history and dark energy, *Phys. Rev. D* **86**, 123504 (2012).
- [59] Ryan E. Keeley, Shahab Joudaki, Manoj Kaplinghat, and David Kirkby, Implications of a transition in the dark energy equation of state for the H_0 and σ_8 tensions, *J. Cosmol. Astropart. Phys.* **12** (2019) 035.
- [60] Shadab Alam *et al.*, Completed SDSS-IV extended Baryon oscillation spectroscopic survey: Cosmological implications from two decades of spectroscopic surveys at the Apache point observatory, *Phys. Rev. D* **103**, 083533 (2021).
- [61] Dante V. Gomez-Navarro, Alexander Mead, Alejandro Aviles, and Axel de la Macorra, Impact of cosmological signatures in two-point statistics beyond the linear regime, *Mon. Not. R. Astron. Soc.* **504**, 3284 (2021).
- [62] A. de la Macorra and E. Almaraz, Theoretical and Observational Constraints of Bound Dark Energy with Precision Cosmological Data, *Phys. Rev. Lett.* **121**, 161303 (2018).
- [63] Erick Almaraz and Axel de la Macorra, Bound dark energy: Towards understanding the nature of dark energy, *Phys. Rev. D* **99**, 103504 (2019).
- [64] Erick Almaraz, Baojiu Li, and Axel de la Macorra, Non-linear structure formation in bound dark energy, *J. Cosmol. Astropart. Phys.* **03** (2020) 016.
- [65] Mariana Jaber-Bravo, Erick Almaraz, and Axel de la Macorra, Imprint of a steep equation of state in the growth of structure, *Astropart. Phys.* **115**, 102388 (2020).
- [66] Axel de la Macorra, Dante V. Gomez-Navarro, Alejandro Aviles, Mariana Jaber, Jorge Mastache, and Erick Almaraz, Cosmological signatures of a rapid diluted energy density, *Phys. Rev. D* **104**, 023529 (2021).
- [67] Antony Lewis, Anthony Challinor, and Anthony Lasenby, Efficient computation of CMB anisotropies in closed FRW models, *Astrophys. J.* **538**, 473 (2000).
- [68] Cullan Howlett, Antony Lewis, Alex Hall, and Anthony Challinor, CMB power spectrum parameter degeneracies in the era of precision cosmology, *J. Cosmol. Astropart. Phys.* **04** (2012) 027.
- [69] Antony Lewis, Efficient sampling of fast and slow cosmological parameters, *Phys. Rev. D* **87**, 103529 (2013).
- [70] Antony Lewis and Sarah Bridle, Cosmological parameters from CMB and other data: A Monte Carlo approach, *Phys. Rev. D* **66**, 103511 (2002).
- [71] Antony Lewis, GetDist: A Python package for analysing Monte Carlo samples (2019), <https://getdist.readthedocs.io>.
- [72] Ryan E. Keeley, Shahab Joudaki, Manoj Kaplinghat, and David Kirkby, Implications of a transition in the dark energy equation of state for the H_0 and σ_8 tensions, *J. Cosmol. Astropart. Phys.* **12** (2019) 035.
- [73] Mariana Jaber and Axel de la Macorra, Probing a steep EoS for dark energy with latest observations, *Astropart. Phys.* **97**, 130 (2018).
- [74] N. Chandrachani Devi, M. Jaber-Bravo, G. Aguilar-Argüello, O. Valenzuela, A. de la Macorra, and H. Velázquez, Non-linear structure formation for dark energy models with a steep equation of state, *J. Cosmol. Astropart. Phys.* **09** (2020) 050.